

DTIC FILE COPY



NASA Contractor Report 181996  
ICASE Report No. 90-14

AD-A227 101

# ICASE

THE INVISCID STABILITY OF SUPERSONIC  
FLOW PAST A SHARP CONE

Peter W. Duck  
Stephen J. Shaw

Contract No. NAS1-18605  
February 1990

Institute for Computer Applications in Science and Engineering  
NASA Langley Research Center  
Hampton, Virginia 23665-5225

Operated by the Universities Space Research Association

DTIC  
ELECTE  
OCT 03 1990  
S E D  
*b*



National Aeronautics and  
Space Administration

Langley Research Center  
Hampton, Virginia 23665-5225

90 10 020

DISTRIBUTION STATEMENT A  
Approved for public release;  
Distribution Unlimited

~~90 03 12 015~~

# THE INVISCID STABILITY OF SUPERSONIC FLOW PAST A SHARP CONE

Peter W. Duck<sup>1</sup> and Stephen J. Shaw  
Department of Mathematics  
University of Manchester

## ABSTRACT

In this paper we consider the laminar boundary layer which forms on a sharp cone in a supersonic freestream, where lateral curvature plays a key role in the physics of the problem.

This flow is then analysed from the point of view of linear, temporal, inviscid stability. Indeed, the basic, non-axisymmetric disturbance equations are derived for general flows of this class, and a so called "triply generalised" inflexion condition is found for the existence of "subsonic" neutral modes of instability. This condition is analogous to the well-known generalised inflexion condition found in planar flows, although in the present case the condition depends on both axial and aximuthal wavenumbers.

Extensive numerical results are presented for the stability problem at a freestream Mach number of 3.8, for a range of streamwise locations. These results reveal that a new mode of instability may occur, peculiar to flows of this type involving lateral curvature.

Additionally, asymptotic analyses valid close to the tip of the cone / far downstream of the cone are presented, and these give a partial (asymptotic) description of this additional mode of instability.

Accession For	
NTIS GRA&I	<input checked="" type="checkbox"/>
DTIC TAB	<input type="checkbox"/>
Unannounced	<input type="checkbox"/>
Justification	
By _____	
Distribution/	
Availability Codes	
Dist	Avail and/or Special
A-1	



<sup>1</sup>This research was supported by the National Aeronautics and Space Administration under NASA Contract No. NAS1-18605 while the second author was in residence at the Institute for Computer Applications in Science and Engineering (ICASE), NASA Langley Research Center, Hampton, VA 23665.

## 1. Introduction and motivation

It is well known that unlike many of their incompressible counterparts, supersonic boundary layers are generally susceptible to inviscid forms of instability; this comment, in particular, applies to Blasius-type boundary layers. The paper which first tackled the problem of stability of supersonic boundary layers, from any kind of rigorous mathematical standpoint was that of Lees and Lin (1946), who presented some extremely important results on the problem, including the importance of the quantity  $\frac{\partial}{\partial y^*} \left[ \rho^* \frac{\partial u^*}{\partial y^*} \right]$  (where  $u^*$  denotes velocity tangential to the surface,  $y^*$  the normal to the surface, and  $\rho^*$  the fluid density), which plays the same role as that of an inflexion point in incompressible flows. In particular at the point where the above expression is zero ( $y^* = y_0^*$ , say), then a neutral mode exists with wavespeed  $u^*(y_0^*)$  (although see the restriction (4.21) later in this paper). Lees and Lin also showed how viscosity played a similar role at a critical layer as in analogous incompressible flow situations. This two-dimensional work was later extended to three-dimensions by Reshotko (1962).

The development of digital computers enabled accurate numerical computations of the problem to be made. One of the earliest was that of Brown (1962), and this was followed by a number of studies by Mack (1963, 1964, 1965a,b, 1969, 1984, 1987a), both of an inviscid (large Reynolds number) and viscous (finite Reynolds number) nature. These computations revealed a further distinction between supersonic and incompressible flows, namely that in the latter case an infinite sequence of modes is possible. These are important, because generally it is one of these "higher" modes that exhibits the largest growth rate according to inviscid, linear stability theory.

In spite of their great practical importance, flows of this type, but involving lateral curvature have received scanty attention over the years.

Duck and Hall (1989a) showed how in supersonic flows, curvature interacting with viscosity could provoke additional instabilities (axisymmetric in form), provided the body radius was below some critical value. Duck and Hall (1989b) then went on to show how a similar effect occurred with non-axisymmetric modes (which, in fact, turn out to be generally more unstable than corresponding axisymmetric modes).

Recently, Duck (1989) (hereafter referred to as I) has shown the influence of curvature on the axisymmetric inviscid stability of supersonic boundary layers, in particular those that form on thin straight circular cylinders. It was found that curvature has a profoundly stabilising effect on these modes. Interestingly, it was shown how curvature altered the generalised inflexion condition described above, and a modified (or "doubly generalised") inflexion condition, involving the radius of curvature was derived.

In the present paper we extend the work of I to non-axisymmetric disturbances which, indeed, turn out to be more important than axisymmetric disturbances considered previously. Further, rather than studying/applying our techniques to the thin straight circular cylinder, we consider a somewhat more practical configuration, namely that of a sharp cone.

To (considerably) facilitate already lengthy and complex computations, following I we assume that the tip of the cone has a finite radius, and that the associated boundary layer on the cone surface is planar at the cone tip. (We expect that far downstream the flow will become planar once again, having utilised the Mangler, 1948, transformation.) Following previous studies in this area, we also ignore the presence of any shocks.

Mack (1987b) has performed some computations for the stability of the flow over a cone in supersonic flow, at finite Reynolds numbers, but found little difference with corresponding planar results. Here, we deliberately allow curvature to occur throughout the study, both in the equations governing the basic flow, and in the disturbance equations.

A few preliminary numerical results of this study have been presented by Duck (1990). Here, we present additional numerical results, and also a number of important asymptotic results related to these calculations.

## 2. Equations of motion and state

The general layout of the problem is shown in Fig. 1. The  $z^*$  axis lies along the cone axis,  $r^*$  denotes the radial coordinate, and  $\theta$  the azimuthal coordinate. The velocity vector  $\underline{v}^*$  has components  $v_1^*$ ,  $v_2^*$  and  $v_3^*$  in the  $r^*$ ,  $\theta$  and  $z^*$  directions respectively. Although we shall be concerned with a basic flow which is independent of  $\theta$  (and with  $v_2^* = 0$ ), when we go on to consider the stability of the flow, we shall be concerned with non-axisymmetric disturbances.

In the cylindrical polar coordinate system as defined above, the full equations of continuity, momentum and energy take on the following forms

(Thompson 1972)

$$\begin{aligned} \frac{\partial \rho^*}{\partial t^*} + \frac{\partial}{\partial r^*} (\rho^* v_1^*) + \frac{1}{r^*} \frac{\partial}{\partial \theta} (\rho^* v_2^*) \\ + \frac{\partial}{\partial z^*} (\rho^* v_3^*) + \frac{\rho^* v_1^*}{r^*} = 0, \end{aligned} \quad (2.1)$$

$$\begin{aligned} \rho^* \left[ \frac{Dv_1^*}{Dt^*} - \frac{(v_2^*)^2}{r^*} \right] = - \frac{\partial p^*}{\partial r^*} + \frac{\partial \Sigma_{r^* r^*}}{\partial r^*} \\ + \frac{1}{r^*} \frac{\partial \Sigma_{r^* \theta}}{\partial \theta} + \frac{\partial \Sigma_{r^* z^*}}{\partial z^*} \\ + \frac{\Sigma_{r^* r^*} - \Sigma_{\theta \theta}}{r^*}, \end{aligned} \quad (2.2)$$

$$\begin{aligned} \rho^* \left[ \frac{Dv_2^*}{Dt^*} + \frac{v_1^* v_2^*}{r^*} \right] = - \frac{1}{r^*} \frac{\partial p^*}{\partial \theta} + \frac{\partial \Sigma_{\theta r^*}}{\partial r^*} \\ + \frac{1}{r^*} \frac{\partial \Sigma_{\theta \theta}}{\partial \theta} + \frac{\partial \Sigma_{\theta z^*}}{\partial z^*} \\ + 2 \frac{\Sigma_{r^* \theta}}{r^*}, \end{aligned} \quad (2.3)$$

$$\rho^* \frac{Dv_3^*}{Dt^*} = - \frac{\partial p^*}{\partial z^*} + \frac{\partial \Sigma_z^* r^*}{dr^*} + \frac{1}{r^*} \frac{\partial \Sigma_r^* \theta}{\partial \theta} + \frac{\partial \Sigma_z^* z^*}{\partial z^*} + \frac{\Sigma_z^* r^*}{r^*} \quad (2.4)$$

$$\rho^* \frac{D}{Dt^*} (c_p T^*) - \frac{Dp^*}{Dt^*} = \Gamma^* + \frac{1}{r^*} \frac{\partial}{\partial r^*} \left( K^* r^* \frac{\partial T^*}{\partial r^*} \right) + \frac{1}{(r^*)^2} \frac{\partial}{\partial \theta} \left( K^* \frac{\partial T^*}{\partial \theta} \right) + \frac{\partial}{\partial z^*} \left( K^* \frac{\partial T^*}{\partial z^*} \right) \quad (2.5)$$

Here  $\rho^*$  is the density of the fluid,  $p^*$  the pressure,  $c_p$  the specific heat (at constant pressure), and  $K^*$  the coefficient of heat conduction. The Eulerian operator is defined as

$$\frac{D}{Dt^*} = \frac{\partial}{\partial t^*} + v_1^* \frac{\partial}{\partial r^*} + \frac{v_2^*}{r^*} \frac{\partial}{\partial \theta} + v_3^* \frac{\partial}{\partial z^*} \quad (2.5)$$

and the viscous stress components, assuming Newtonian flow are defined to be

$$\Sigma_r^* r^* = 2\mu^* \frac{\partial v_1^*}{dr^*} + \lambda^* \nabla \cdot \underline{v}^* \quad (2.6)$$

$$\Sigma_{\theta\theta} = 2\mu^* \left[ \frac{1}{r^*} \frac{\partial v_2^*}{\partial \theta} + \frac{v_1^*}{r^*} \right] + \lambda^* \nabla \cdot \underline{v}^* \quad (2.7)$$

$$\Sigma_z^* z^* = 2\mu^* \frac{\partial v_3^*}{\partial z^*} + \lambda^* \nabla \cdot \underline{v}^* \quad (2.8)$$

$$\Sigma_r^* \theta = \Sigma_{\theta r^*} = \mu^* \left[ \frac{1}{r^*} \frac{\partial v_1^*}{\partial \theta} + r^* \frac{\partial}{\partial r^*} \left( \frac{v_2^*}{r^*} \right) \right] \quad (2.9)$$

$$\Sigma_{\theta z^*} = \Sigma_z^* \theta = \mu^* \left[ \frac{\partial v_2^*}{\partial z^*} + \frac{1}{r^*} \frac{\partial v_3^*}{\partial \theta} \right] \quad (2.10)$$

$$\Sigma_z^* r^* = \Sigma_r^* z^* = \mu^* \left[ \frac{\partial v_3^*}{\partial r^*} + \frac{\partial v_1^*}{\partial z^*} \right] \quad (2.11)$$

The dispersion function  $\Gamma^*$  in (2.5) is given by

$$\begin{aligned} \Gamma^* = 2\mu & \left[ D_{r^*r^*}^2 + D_{\theta\theta}^2 + D_{z^*z^*}^2 \right. \\ & \left. + 2 D_{r^*\theta}^2 + 2 D_{z^*\theta}^2 + 2 D_{z^*r^*}^2 \right] \\ & + (\lambda^* - \frac{2}{3} \mu^*) (\nabla \cdot \mathbf{v}^*)^2. \end{aligned} \quad (2.12)$$

Here the 'D' terms are the components of the rate-of-deformation tensor, for example

$$D_{\theta\theta} = \frac{1}{r^*} \frac{\partial v_2^*}{\partial \theta} + \frac{v_1^*}{r^*}, \quad (2.13)$$

$$D_{z^*\theta} = \frac{1}{2} \left[ \frac{\partial v_2^*}{\partial z^*} + \frac{1}{r^*} \frac{\partial v_3^*}{\partial \theta} \right]. \quad (2.14)$$

The coefficients  $\mu^*$  and  $\lambda^*$  above denote the first coefficient of viscosity and bulk viscosity respectively (which are expected to be functions of temperature).

The equation of state is taken to be that pertaining to a perfect gas, i.e.

$$p^* = \rho^* R^* T^*, \quad (2.15)$$

where  $R^*$  is the gas constant.

With reference to Fig. 1, the surface of the cone is taken to lie along  $r^* = a^* + \lambda_1 z^*$ ,  $z^* > 0$ , (later, important assumptions regarding the size of the slope parameter will be made), and so on this surface we require

$$v_1^* = v_2^* = v_3^* = 0. \quad (2.16)$$

If the surface of the cone is insulated then the following additional boundary condition must be imposed

$$\frac{\partial \Gamma^*}{\partial n^*} = 0, \quad (2.17)$$

(where  $n^*$  denotes an outwards normal to the wall). In the case of heated/

cooled walls, then the condition

$$T^* = T_w^* \quad (2.18)$$

must be imposed at the surface.

Conditions remain to be specified at  $z^* = 0$ ; for this we follow I (precisely) by assuming that the boundary layer at this location has zero thickness, enabling planar conditions to be imposed at this position. Assuming the cone to be slender, then the far-field conditions are taken to be uniform, with

$$v_1^* = v_2^* = 0 \quad (2.19)$$

$$v_3^* = U_\infty^* \quad (2.20)$$

$$T^* = T_\infty^* \quad (2.21)$$

(Indeed, in the case of non-slender cones, if the shock wave is attached, downstream of the shock the external flow is irrotational, and there is also a constant slip velocity at the surface of the cone.) We next go on to derive the basic (boundary-layer) flow on the surface of the cone, assuming curvature plays a key role in the physics of the problem.

### 3. The boundary layer flow

We define our Reynolds number on the tip radius of the cone,  $a^*$ , as follows

$$Re = \frac{U_\infty^* a^* \rho_\infty^*}{\mu_\infty^*}, \quad (3.1)$$

and this will be taken to be large throughout this paper. As noted previously, the basic flow is taken to be independent of  $\theta$ , and has no azimuthal velocity component (i.e.  $v_2^* = 0$ ).

It is now convenient to introduce non-dimensional parameters as follows  
( $v_1, v_3, r, z, T, \rho, \mu$ ) =

$$\left( \frac{Re v_1^*}{U_\infty^*}, \frac{v_3^*}{U_\infty^*}, \frac{r^*}{a^*}, \frac{z^*}{Re a^*}, \frac{T^*}{T_\infty^*}, \frac{\rho^*}{\rho_\infty^*}, \frac{\mu^*}{\mu_\infty^*} \right). \quad (3.2)$$

A key element of this paper (as in I) is the inclusion of curvature terms in the governing equations to leading order. If this is to be the case, then we must have that

$$\lambda_1 = \text{Re}^{-1} \bar{\lambda}$$

where  $\bar{\lambda} = O(1)$ , (3.3)

implying a slender cone.

The leading order governing equations may then be written (assuming  $\text{Re} \rightarrow \infty$ )

$$\frac{\partial}{\partial r} \left( \frac{v_1}{r} \right) + \frac{v_1}{r^2} + \frac{\partial}{\partial z} \left( \frac{v_3}{r} \right) = 0 \quad (3.4)$$

$$\frac{\partial p}{\partial r} = 0 \quad (3.5)$$

$$v_1 \frac{\partial v_3}{\partial r} + v_3 \frac{\partial v_3}{\partial z} = \frac{T}{r} \frac{\partial}{\partial r} \left[ r \mu \frac{\partial v_3}{\partial r} \right] \quad (3.6)$$

$$v_1 \frac{\partial T}{\partial r} + v_3 \frac{\partial T}{\partial z} = \mu T (\gamma - 1) M_\infty^2 \left[ \frac{\partial v_3}{\partial r} \right]^2 + \frac{T}{r} \frac{\partial}{\partial r} \left[ \frac{r \mu}{\sigma} \frac{\partial T}{\partial r} \right], \quad (3.7)$$

where the result

$$\rho = \frac{1}{T} \quad (3.8)$$

has been used,  $\sigma$  is the Prandtl number, namely

$$\sigma = \frac{\mu_\infty^* c_p}{K^*} \quad (3.9)$$

(which is taken to be a constant in this paper),  $\gamma$  denoting the ratio of specific heats, and  $M_\infty$  is the freestream Mach number, namely

$$M_\infty = U_\infty^* / (\gamma R^* T_\infty^*)^{1/2}. \quad (3.10)$$

The boundary conditions to be applied to this system are

$$\begin{aligned} v_1 = v_3 = 0 & \quad \text{on} \quad r = 1 + \bar{\lambda} z, \\ v_3 \rightarrow 1, \quad T \rightarrow 1 & \quad \text{as} \quad r \rightarrow \infty, \end{aligned} \quad (3.11)$$

together with a wall temperature condition; in the case of insulated walls,

(to leading order)

$$\frac{\partial T}{\partial r} = 0 \quad \text{on} \quad r = 1 + \bar{\lambda} z, \quad (3.12)$$

whilst in the case of heated/cooled surfaces

$$T = T_w \quad \text{on} \quad r = 1 + \bar{\lambda} z. \quad (3.13)$$

To close the problem, a viscosity/temperature law is required. For the purposes of this paper we take the linear Chapman law (Stewartson 1964), namely

$$\mu = CT \quad (3.14)$$

where  $C$  is taken to be constant (although as noted in I, there would be no conceptual difficulties in taking more complex variations of viscosity with temperature).

If we write

$$\begin{aligned} v_1 &= C \bar{v}_1, \\ z &= C \bar{z}, \\ \bar{\lambda} &= C\lambda, \end{aligned} \quad (3.15)$$

whilst retaining other terms, then the system (3.4) - (3.7) becomes

$$\frac{\partial}{\partial r} \left[ \frac{\bar{v}_1}{T} \right] + \frac{\bar{v}_1}{rT} + \frac{\partial}{\partial \bar{z}} \left[ \frac{v_3}{T} \right] = 0, \quad (3.16)$$

$$\frac{\partial p}{\partial r} = 0, \quad (3.17)$$

$$\bar{v}_1 \frac{\partial v_3}{\partial r} + v_3 \frac{\partial v_3}{\partial \bar{z}} = \frac{T}{r} \frac{\partial}{\partial r} \left[ rT \frac{\partial v_3}{\partial r} \right], \quad (3.18)$$

$$\begin{aligned} \bar{v}_1 \frac{\partial T}{\partial r} + v_3 \frac{\partial T}{\partial \bar{z}} &= T^2 (\gamma-1) M_\infty^2 \left[ \frac{\partial v_3}{\partial r} \right]^2 \\ &+ \frac{T}{r} \frac{\partial}{\partial r} \left[ \frac{rT}{\sigma} \frac{\partial T}{\partial r} \right], \end{aligned} \quad (3.19)$$

whilst the wall boundary conditions are to be applied on

$$r = 1 + \lambda \bar{z}.$$

As described previously we assume planar conditions prevail at  $z = 0$ , where the boundary layer is taken to have zero thickness. The problem is thus singular at  $z = 0$ , and consequently scaled variables must be introduced in order to (numerically) solve the system (3.16) - (3.19) accurately. Specifically we write

$$\begin{aligned}\bar{v}_1 &= \zeta^{-1} \hat{v}_1(\eta, \zeta), \\ v_3 &= \hat{v}_3(\eta, \zeta), \\ T &= \hat{T}(\eta, \zeta),\end{aligned}\quad (3.20)$$

where

$$\zeta = z^{\frac{1}{2}}, \quad (3.21)$$

$$\text{and } \eta = (r - 1 - \lambda\zeta^2)/\zeta. \quad (3.22)$$

The quantities with a hat are then expected to behave regularly as  $\zeta \rightarrow 0$ , and indeed approach the planar solution. Equations (3.16) - (3.19) now take the following form

$$\frac{\partial}{\partial \eta} \left[ \frac{\hat{v}_1}{r} \right] + \frac{\zeta \hat{v}_1}{r} + \frac{\zeta}{2} \frac{\partial}{\partial \zeta} \left[ \frac{\hat{v}_3}{r} \right] - \left[ \lambda\zeta + \frac{\eta}{2} \right] \frac{\partial}{\partial \eta} \left[ \frac{\hat{v}_3}{r} \right] = 0, \quad (3.23)$$

$$\frac{\partial p}{\partial \eta} = 0, \quad (3.24)$$

$$v_1 \frac{\partial \hat{v}_3}{\partial \eta} + \frac{\zeta \hat{v}_3}{2} \frac{\partial \hat{v}_3}{\partial \zeta} - \hat{v}_3 \left[ \lambda\zeta + \frac{\eta}{2} \right] \frac{\partial \hat{v}_3}{\partial \eta} = \frac{\hat{T}}{r} \frac{\partial}{\partial \eta} \left[ rT \frac{\partial \hat{v}_3}{\partial \eta} \right], \quad (3.25)$$

$$\begin{aligned}\hat{v}_1 \frac{\partial \hat{T}}{\partial \eta} + \frac{\zeta \hat{v}_3}{2} \frac{\partial \hat{T}}{\partial \zeta} - \hat{v}_3 \left[ \lambda\zeta + \frac{\eta}{2} \right] \frac{\partial \hat{T}}{\partial \eta} \\ = \hat{T}^2 (\gamma - 1) M_\infty^2 \left[ \frac{\partial \hat{v}_3}{\partial \eta} \right]^2 + \frac{\hat{T}}{r} \frac{\partial}{\partial \eta} \left[ \frac{r\hat{T}}{\sigma} \frac{\partial \hat{T}}{\partial \eta} \right].\end{aligned}\quad (3.26)$$

Here of course

$$r = 1 + \lambda \zeta^2 + \zeta \eta . \quad (3.27)$$

The boundary conditions in terms of these variables are

$$\begin{aligned} \hat{v}_1 = \hat{v}_3 = 0 \quad \text{on} \quad \eta = 0 \\ \hat{v}_3 \rightarrow 1, \quad \hat{T} \rightarrow 1 \quad \text{as} \quad \eta \rightarrow \infty . \end{aligned} \quad (3.28)$$

In the case of insulated walls, the additional surface condition is

$$\frac{\partial \hat{T}}{\partial \eta} = 0 \quad \text{on} \quad \eta = 0 , \quad (3.29)$$

whilst for heated/cooled walls,

$$\hat{T} = T_w \quad \text{on} \quad \eta = 0 . \quad (3.30)$$

Setting  $\zeta = 0$  reduces the system to an ordinary differential system (corresponding to the planar case) as in I in the same limit (indeed, setting  $\lambda = 0$  reduces (3.23) - (3.26) to the corresponding system considered in I). The solution of the ordinary differential system at  $\zeta = 0$  then provides the initial conditions for a (straightforward) Crank-Nicolson scheme in  $\zeta$ , identical to that used in I. For the purposes of this paper, we shall focus our attention on the insulated wall case (although the heated/cooled case may be treated in exactly the same manner). Distributions of wall temperature with axial coordinate  $\zeta (= z \frac{1}{2})$  are shown in Fig. 2a ( $M_\infty = 2.8$ ) and Fig. 2b ( $M_\infty = 3.8$ ), and the corresponding distributions of wall shear  $\hat{v}_{3\eta}|_{\eta=0}$  are shown in Fig. 3a ( $M_\infty = 2.8$ ) and Fig. 3b ( $M_\infty = 3.8$ ).

In all cases, these distributions are quite different to the corresponding  $\lambda = 0$  distributions (i.e. the distributions on a straight circular cylinder) as found in I, where at both  $M_\infty = 2.8$  and  $3.8$  a monotonic decrease in values was found. It is also quite clear that the results evolve from the planar case, to the far downstream limit, as predicted by the Mangler Transformation (Mangler 1946, Stewartson 1964), namely

$$\begin{aligned} \hat{v}_{3\eta} \Big|_{\eta=0, \zeta \rightarrow \infty} &\longrightarrow \sqrt{3} \hat{v}_{3\eta} \Big|_{\eta=0, \zeta=0} \\ \hat{T} \Big|_{\eta=0, \zeta \rightarrow \infty} &\longrightarrow \hat{T} \Big|_{\eta=0, \zeta=0} . \end{aligned} \quad (3.31)$$

In the following section we go on to investigate the stability of flows of this class, subject to small amplitude inviscid disturbances.

#### 4. Inviscid stability of the flow

##### 4.1 Disturbance equations

In this section we derive the disturbance equations relevant to small amplitude disturbances in any supersonic axisymmetric boundary layer type flow. In 1, just axisymmetric disturbances were considered; here we consider the more general case of non-axisymmetric perturbations of the flow.

We consider disturbances whose wavelength in the axial direction ( $1/\bar{\alpha}$ ) is comparable to the (tip) radius of the cone. Specifically, at a fixed  $\bar{z}$  station we write

$$\begin{aligned} v_1^* &= \delta \bar{\alpha} U_\infty^* \tilde{v}_1(r) E + O(\delta^2) , \\ v_2^* &= \delta U_\infty^* \tilde{v}_2(r) E + O(\delta^2) , \\ v_3^* &= U_\infty^* [W_0(r) + \delta \tilde{v}_3(r) E] + O(\delta^2) , \\ T^* &= T_\infty^* [T_0(r) + \delta \tilde{T}(r) E] + O(\delta^2) , \\ \rho^* &= \rho_\infty^* \left[ \frac{1}{T_0}(r) + \delta \tilde{\rho}(r) E \right] + O(\delta^2) , \\ p &= \rho_\infty^* R^* T_\infty^* [1 + \delta \tilde{p}(r) E] + O(\delta^2) , \end{aligned} \quad (4.1)$$

$$\text{where } E = \exp [i \bar{\alpha} (\hat{z} - ct) + in \theta] , \quad (4.2)$$

and  $\delta$  is the scale of the disturbance (taken to be diminishingly small).

whilst

$$\begin{aligned}
 t &= (U_\infty^*/a^*) t^* , \\
 \hat{z} &= z^*/a^* \\
 W_0(r) &= \hat{v}_3 (r, \bar{z}) , \\
 T_0(r) &= \hat{T} (r, \bar{z}) ,
 \end{aligned} \tag{4.3}$$

where  $\hat{v}_3$  and  $\hat{T}$  are found from the computations in the previous section.

Substituting (4.1) into (2.1) - (2.4) and taking the  $O(5)$  terms of leading order in  $Re$  yields the following linear system

$$\begin{aligned}
 -ic\tilde{p} + \frac{i\tilde{v}_3}{T_0} + \frac{1}{rT_0} \tilde{v}_1 + \frac{\tilde{v}_1 r}{T_0} + in \frac{\tilde{v}_2}{r T_0 \alpha} \\
 + i W_0 \tilde{p} - \tilde{v}_1 \frac{T_0 r}{T_0^2} = 0 ,
 \end{aligned} \tag{4.4}$$

$$-\frac{ic}{T_0} \tilde{v}_3 + i \frac{W_0 \tilde{v}_3}{T_0} + \tilde{v}_1 \frac{W_0 r}{T_0} = -\frac{i\tilde{p}}{\gamma M_\infty^2} , \tag{4.5}$$

$$-\frac{ic}{T_0} \tilde{v}_2 + i \frac{W_0 \tilde{v}_2}{T_0} = -\frac{in\tilde{p}}{\gamma M_\infty^2 \alpha r} , \tag{4.6}$$

$$-i \frac{\alpha^2 c}{T_0} \tilde{v}_1 + i \frac{\alpha^2 W_0 \tilde{v}_1}{T_0} = -\frac{\tilde{p} r}{\gamma M_\infty^2} , \tag{4.7}$$

$$\frac{1}{T_0} \left[ -ic\tilde{T} + iW_0\tilde{T} + \tilde{v}_1 T_0 r \right] + \left( \frac{\gamma-1}{\gamma} \right) (ic\tilde{p} - iW_0\tilde{p}) = 0 . \tag{4.8}$$

The perturbation equation of state is

$$\tilde{p} = T_0 \tilde{\rho} + \frac{\tilde{T}}{T_0} . \tag{4.9}$$

After some algebra, this system may be reduced to the following two equations

$$\begin{aligned}
 \tilde{v}_1 r + \frac{1}{r} \tilde{v}_1 - \frac{W_0 r}{(W_0 - c)} \tilde{v}_1 \\
 = \frac{i\tilde{p}}{\gamma M_\infty^2 (W_0 - c)} \left[ T_0 \left[ 1 + \frac{n^2}{\alpha^2 r^2} \right] - M_\infty^2 (W_0 - c)^2 \right] ,
 \end{aligned} \tag{4.10}$$

$$\frac{i\alpha^2}{T_0} (W_0 - c) \tilde{v}_1 = -\frac{1}{\gamma M_\infty^2} \tilde{p} r , \tag{4.11}$$

a result also to be found in the work on the stability of jets by Michalke (1971). Writing

$$\tilde{v}_1 = \zeta \varphi, \quad \alpha = \alpha/\zeta, \quad (4.12)$$

gives

$$\begin{aligned} & \varphi_\eta + \frac{\zeta}{1+\lambda\zeta^2+\zeta\eta} \varphi - \frac{W_{0\eta}}{W_0-c} \varphi \\ &= \frac{i\tilde{p}}{\gamma M_\infty^2 (W_0-c)} \left\{ T_0 \left[ 1 + \frac{n^2 \zeta^2}{\alpha^2 (1+\lambda\zeta^2 + \zeta\eta)^2} \right] - M_\infty^2 (W_0-c)^2 \right\}. \end{aligned} \quad (4.13)$$

together with

$$i\alpha^2 (W_0-c) \frac{\varphi}{T_0} = - \frac{\tilde{p}_\eta}{\gamma M_\infty^2}. \quad (4.14)$$

These equations may be combined to eliminate  $\tilde{p}$  to give

$$\begin{aligned} & \frac{d}{d\eta} \left\{ \frac{(W_0-c) \left[ \varphi_\eta + \frac{\zeta}{1+\lambda\zeta^2+\zeta\eta} \varphi \right] - W_{0\eta} \varphi}{T_0 \left[ 1 + \frac{n^2 \zeta^2}{\alpha^2 (1+\lambda\zeta^2 + \zeta\eta)^2} \right] - M_\infty^2 (W_0-c)^2} \right\} \\ &= \frac{\alpha^2}{T_0} (W_0-c) \varphi. \end{aligned} \quad (4.15)$$

Alternatively  $\varphi$  may be eliminated to give

$$\begin{aligned} & \tilde{p} \left\{ (W_0-c)^2 M_\infty^2 - T_0 \left[ 1 + \frac{\zeta^2 n^2}{\alpha^2 (1+\lambda\zeta^2 + \zeta\eta)^2} \right] \right\} \\ &= \left\{ W_{0\eta} - \frac{\zeta(W_0-c)}{1+\lambda\zeta^2+\zeta\eta} \right\} \frac{\tilde{p}_\eta T_0}{\alpha^2 (W_0-c)} \\ &- (W_0-c) \frac{d}{d\eta} \left\{ \frac{T_0 \tilde{p}_\eta}{\alpha^2 (W_0-c)} \right\} \end{aligned} \quad (4.16)$$

These equations reduce naturally to the system considered in I by setting  $n = 0$  (i.e. axisymmetric disturbances) and  $\lambda = 0$  (zero cone angle).

The boundary conditions to be applied to the above systems are that

$$\varphi = \tilde{p}_\eta = 0 \quad \text{on} \quad \eta = 0, \quad (4.17)$$

together with

$$\varphi \sim \frac{1}{2} \varphi_\infty \left\{ K_{n+1}(\hat{\eta}) + K_{|n-1|}(\hat{\eta}) \right\}, \quad (4.18)$$

$$\tilde{p} \sim \mp \frac{\varphi_\infty M_\infty^2 i \alpha \gamma (1-c) K_n(\hat{\eta})}{[1 - M_\infty^2 (1-c)^2]^{\frac{1}{2}}}, \quad (4.19)$$

$$\text{where } \hat{\eta} = \pm \alpha [1 - M_\infty^2 (1-c)^2]^{\frac{1}{2}} \left[ \frac{1}{\zeta} + \lambda \zeta + \eta \right]; \quad (4.20)$$

here the appropriate sign is chosen to ensure that the real part of  $\hat{\eta}$  is positive as  $\eta \rightarrow \infty$ , to ensure boundedness. Equations (4.15) together with (4.17) and (4.18) (or (4.16) together with (4.17) and (4.19), or (4.13), (4.14) together with (4.17), (4.18), (4.19)) constitute an eigenvalue problem; here, we consider just the temporal problem, i.e. given  $n$  and  $\alpha$  (real), to find  $c$  (generally complex). The problem was treated numerically using a Runge-Kutta method based on (4.13) and (4.14), shooting inwards from some suitably large value of  $\eta$ , with contour indentation in the manner described in I.

#### 4.2 The "triple generalised inflexion condition"

In I, a condition for the existence of so called inviscid, neutral, axisymmetric mode, i.e. those for which

$$1 - 1/M_\infty < c < 1 + 1/M_\infty, \quad (4.21)$$

implying disturbances that decay as  $\eta \rightarrow \infty$ , was derived. Here, we go on to derive the corresponding condition for non-axisymmetric modes.

If we multiply (4.15) by  $\varphi^*$  (where an asterisk denotes a complex conjugate), and subtract from the resulting equation its complex conjugate, then the following equation is obtained

$$\begin{aligned} & \frac{\varphi^*}{W_0 - c} \frac{d}{d\eta} \left\{ \frac{(W_0 - c) \left( \varphi_\eta + \frac{1}{r} \varphi \right) - W_{0\eta} \varphi}{\chi} \right\} \\ &= \frac{\varphi}{W_0 - c^*} \frac{d}{d\eta} \left\{ \frac{(W_0 - c^*) \left( \varphi_\eta^* + \frac{1}{r} \varphi^* \right) - W_{0\eta} \varphi^*}{\chi^*} \right\}, \end{aligned} \quad (4.22)$$

where we have written

$$\chi = T_0 \left\{ 1 + \frac{n^2}{a^2 r^2} \right\} - M_\infty^2 (W_0 - c)^2, \quad (4.23)$$

$$\text{and } r = (1 + \lambda \zeta^2 + \zeta \eta) / \zeta. \quad (4.24)$$

After some algebra, (4.22) can be written as

$$\begin{aligned} & \varphi^* \frac{d}{d\eta} \left\{ \frac{\varphi_\eta + \frac{1}{r} \varphi}{\chi} \right\} - \varphi \frac{d}{d\eta} \left\{ \frac{\varphi_\eta^* + \frac{1}{r} \varphi^*}{\chi^*} \right\} \\ &= r \varphi \varphi^* \left\{ \frac{1}{W_0 - c} \frac{d}{d\eta} \left[ \frac{W_{0\eta}}{\chi r} \right] - \frac{1}{W_0 - c^*} \frac{d}{d\eta} \left[ \frac{W_{0\eta}}{\chi^* r} \right] \right\}. \end{aligned} \quad (4.25)$$

$$\text{Writing } c = c_r + i c_i, \quad (4.26)$$

then the neutral state corresponds to  $c_i \rightarrow 0$ .

In this limit, (4.25) may be written

$$\begin{aligned} & \frac{d}{d\eta} \left\{ \frac{r \left[ \varphi^* \left( \varphi_\eta + \frac{1}{r} \varphi \right) - \varphi \left( \varphi_\eta^* + \frac{1}{r} \varphi^* \right) \right]}{\chi} \right\} \\ &= 2i \frac{r^2 |\varphi|^2 c_i}{|W_0 - c|^2} \frac{d}{d\eta} \left\{ \frac{W_{0\eta}}{\chi r} \right\} \end{aligned} \quad (4.27)$$

Following the arguments used in 1, if the neutral mode is subsonic, and satisfies the impermeability boundary condition on  $\eta = 0$ , then to avoid any contradiction the right-hand-side must be zero at the critical point where  $W_0 = c$  namely  $\eta = \eta_i$ ; this requires (recasting the equation in terms of the original variables)

$$\frac{d}{d\eta} \left\{ \frac{W_{0\eta}}{To [1+\lambda\zeta^2 + \zeta\eta] \left[ 1 + \frac{n^2 \zeta^2}{\alpha^2 (1+\lambda\zeta^2+\zeta\eta)^2} \right]} \right\}_{\eta = \eta_i} = 0 \quad (4.28)$$

This result represents a further generalisation of the so-called "doubly generalised inflexion condition" (or a "triply generalised inflexion condition!"); setting  $n = \lambda = 0$  in (4.28) retrieves the corresponding result found in I. Note that in the general result for any shape of cone surface described by

$$r = 1 + \lambda f(\zeta) \quad (4.29)$$

merely requires the " $\lambda\zeta^2$ " in (4.28) to be replaced by " $\lambda f(\zeta)$ ".

### 5. Numerical Results

There are clearly many choices of parameters to be made in this study. The strategy here will be to carry out a detailed study for one choice of Prandtl number (0.72), ratio of specific heats (1.4), cone angle ( $\lambda = 1$ ) and Mach number ( $M_\infty = 3.8$ ) for insulated wall conditions; results are shown in Figs. 4-11. Results for  $c_i$  are presented for a range of values of  $n$ , at fixed values of  $\zeta$ . Specifically results for  $\zeta = 0.01$  (Fig. 4),  $\zeta = 0.05$  (Fig. 5),  $\zeta = 0.1$  (Fig. 6),  $\zeta = 0.2$  (Fig. 7),  $\zeta = 1$  (Fig. 8),  $\zeta = 5$  (Fig. 9),  $\zeta = 20$  (Fig. 10) and  $\zeta = 75$  (Fig. 11). In these figures we just concentrate on growing/neutral modes. All results may be regarded as being independent of numerical grid. In a number of cases the distributions are shown on two figures - this is to increase the resolution of certain features of the distribution in regions of small growth rates. In all these figures, the  $n = 0$  results are delineated by a solidus, the  $n = 1$  results by - - - -,  $n = 2$  results by — - — - —,  $n = 3$  results by — - - — - - — and  $n = 4$  results by ..... Neutral points are also marked on the axes.

The corresponding planar results are shown in Mack (1965, 1987a) and I; the important feature in this case is the existence of two primary instability modes (and others, but of considerably smaller growth rate), with the largest growth rate being associated with the so called "second mode".

Figure 4 shows distributions at the location  $\zeta = 0.01$ , for  $n = 0, 1, 2, 3, 4$ . The axisymmetric ( $n = 0$ ) results are very similar to Mack's planar results described above (and the axisymmetric results for the circular cylinder case close to the leading edge, as considered in I). The first mode extends from close to  $\alpha = 0$  (where  $c_r$  is approximately  $1 - 1/M_\infty$  up to  $\alpha \approx 0.14$  (terminating at a doubly generalised inflexion point); we shall refer to modes of this general type as mode I. A second mode originates at  $\alpha \approx 0.24$  (where  $c_r = 1$ , and hence may be regarded as a generalised inflexional neutral mode, with the critical layer occurring in the freestream) and terminates at around  $\alpha \approx 0.4$  (which corresponds to a second doubly generalised inflexional neutral mode); we refer to modes of this general type as mode II.

In some ways the corresponding  $n = 1$  results for  $c_i$  (also shown in Fig. 4) are very similar to the axisymmetric case. However a third mode is seen to develop, not present in the corresponding axisymmetric (and indeed planar) results. One important distinction between the  $n = 0$  results and those for  $n \neq 0$  emerges in the limit as  $\alpha \rightarrow 0$ , for which  $c_i \rightarrow 0$  if  $n \neq 0$  (the limit as  $\alpha \rightarrow 0$ ,  $\zeta = O(1)$  is considered in Appendix A), although of course the temporal growth/decay rate  $\alpha c_i$  is nonetheless zero at  $\alpha = 0$ . We shall refer to this additional mode as mode  $I_A$ . As  $\alpha$  increases, mode  $I_A$  rapidly disappears, terminating at a supersonic neutral point (i.e. where  $c_r < 1 - 1/M_\infty$ ). As  $\alpha$  increases, a further neutral mode soon emerges, at a second (supersonic) neutral point; this mode is of the class I type described previously. Thereafter, as  $\alpha$  is increased

further, the  $n = 1$  distribution closely resembles the  $n = 0$  results.

The  $n = 2$  distribution is qualitatively similar to those of  $n = 1$ ; however when  $n = 3$ , modes  $I_A$  and  $I$  are seen to amalgamate, although mode  $II$  remains quantitatively similar to the mode  $II$  results of the previous  $n$  values. In the case of  $n = 4$ , mode  $I$  admits further enhanced growth rates although it is still mode  $II$  that possesses the largest growth rate ( $\propto c_i$ ).

It is not surprising that at  $\zeta = 0.01$  results very similar to corresponding planar results are obtained, since curvature, generally, will play a minor role in the physics here; indeed a crude examination of (4.15) suggests that as  $\zeta \rightarrow 0$ , the corresponding planar Rayleigh equation is attained. However, as  $\alpha \rightarrow 0$  and  $\zeta \rightarrow 0$  a non-uniformity is present; this aspect is taken up in some detail in the following section, where further light is shed on the additional mode  $I_A$ .

Figure 5 shows results for  $c_i$  at  $\zeta = 0.05$ . The axisymmetric mode exhibits the same general features as the corresponding mode shown on Fig. 4, although both modes  $I$  and  $II$  have diminished growth rates. In the case of  $n = 1$ , it is to be noted that mode  $I_A$  has (already) amalgamated with mode  $I$ , whilst mode  $II$  has significantly reduced growth rates compared to the  $\zeta = 0.01$  value, although this remains the more dangerous mode. In the case of  $n = 2$ , the combined modes  $I$  and  $I_A$  exhibit an enhanced growth rate when compared with the  $\zeta = 0.01$  station, whilst comparing corresponding mode  $II$ s, we note that the growth rate is diminished; indeed, for  $n = 2$ , the maximum growth rate of the two modes is comparable. In the case of  $n = 3$ , the first mode again is more dangerous compared to the corresponding mode at  $\zeta = 0.01$ , and this trend is repeated by the  $n = 4$  results, although this value of  $n$  indicates that an increase in  $n$  is causing a decrease in growth rate.

Figure 6 shows results at the  $\zeta = 0.10$  location. These confirm the trends observed previously, of a less unstable mode II, whilst the (combined) mode I has a maximum growth rate comparable to mode II; although it appears that the  $n = 0$  mode II remains the most unstable.

Figure 7a shows  $c_i$  versus  $\alpha$  distribution at  $\zeta = 0.20$ . In this case mode II is barely visible, and so Fig. 7b shows these modes on a larger scale. Interestingly, it seems to be the  $n = 2$  mode I that exhibits the largest growth rate and is consequently the most important.

Figure 8a shows  $c_i$  distributions at  $\zeta = 1$ . Again, because of the very small growth rates, mode II is shown on an enhanced scale in Fig. 8b. Note that at this axial location the  $n = 0$  and  $n = 4$  (and above) cases do not possess an unstable mode I at all (whilst the  $n = 4$  mode II has such small growth rates that it is not visible even on the scale of Fig. 8b). Overall, it is the  $n = 1$  mode I which is the most dangerous.

Moving further downstream to  $\zeta = 5$  (Figs. 9a, 9b) we see a "recovery" in the maximum growth rate of mode II. Indeed, these results show some resemblance to the  $\zeta = 0.2$  shown in Figs. 7a, 7b. This is not too surprising, given that, on account of the Mangler transformation (Mangler 1948, Stewartson 1964), results as  $\zeta \rightarrow \infty$  mirror those as  $\zeta \rightarrow 0$  (except for a multiplicative factor of  $\sqrt{3}$  in  $\alpha$ ).

This trend is confined in Fig. 10 for  $\zeta = 20$ , which may be compared directly to the  $\zeta = 0.05$  results of Fig. 5. Notice, in particular, the re-emergence of mode  $I_A$  for  $n = 1$ .

Figure 11 shows results at the furthest downstream location studied, namely  $\zeta = 75$ . The  $n = 0$  modes now correspond closely with the planar results of Mack (1984, 1987a for example), (with the factor  $\sqrt{3}$  multiplying  $\alpha$ ), whilst mode  $I_A$  is visible for  $n = 1$  and 2, and the union of modes  $I_A$  and I is clearly seen in the case of  $n = 3$ .

Thus to summarise, these results, which will guide us in certain asymptotic aspects in the following section, we observe the following general features of the stability of the flow: (i) results as  $\zeta \rightarrow \infty$  mirror those as  $\zeta \rightarrow 0$ , except for a multiplication factor of  $\sqrt{3}$ ; (ii) Lateral curvature has a strongly stabilising influence on mode II, together with the axisymmetric mode I (this is in accord with the results found in I); (iii) there emerges a third mode,  $I_A$ , as  $\alpha \rightarrow 0$ , with  $\zeta \rightarrow 0$  or  $\zeta \rightarrow \infty$ , in the case of  $n \neq 0$ .

In the following section we go on to consider various asymptotic limits of the system (4.15) (or (4.16)), guided partly by the observations made above.

## 6. Asymptotic Results

In this section we consider a number of asymptotic limits of the stability problem, to give us a better understanding of the details of the numerical results described in the previous section.

Perhaps the most intriguing feature of these numerical results is the emergence of an additional mode as  $\zeta \rightarrow 0$  (or  $\zeta \rightarrow \infty$ ) with  $\alpha \rightarrow 0$ . We investigate this feature first.

### 6.1 $\zeta \rightarrow 0$ , $\alpha = 0(\zeta)$ or $\zeta \rightarrow \infty$ , $\alpha = 0(\zeta^{-1})$

Since the problem as posed is basically equivalent as  $\zeta \rightarrow 0$  and  $\zeta \rightarrow \infty$ , we consider just the former limit, and later we describe, briefly, how the results for the latter limit can be simply inferred.

As noted in Section 5, as  $\zeta \rightarrow 0$ , (4.15) is seen to generally reduce to the planar system treated by Mack (1984, 1987a for example). However this will no longer be the case if  $\alpha = 0(\zeta)$ , since then the denominator on the left-hand-side of (4.15) no longer reduces to the planar result.

Specifically, let us write (consistent with (4.12))

$$\alpha = \zeta \hat{\alpha} , \quad (6.1)$$

where it is assumed  $\alpha = O(1)$  as  $\zeta \rightarrow 0$ . The results for mode  $I_A$  shown in the previous section, together with other results obtained by the authors indicate that as  $\zeta \rightarrow 0$ ,  $c \rightarrow 0$  also.

Partly guided by this, if  $\eta = O(1)$  we set

$$c = \zeta c_1 + \zeta^2 c_2 + \zeta^3 c_3 + \dots \quad (6.2)$$

$$\varphi = \varphi_0(\eta) + \zeta \varphi_1(\eta) + \zeta^2 \varphi_2(\eta) + \zeta^3 \varphi_3(\eta) + \dots \quad (6.3)$$

$$W_0 = W_{00}(\eta) + \zeta W_{01}(\eta) + \zeta^2 W_{02}(\eta) + \zeta^3 W_{03}(\zeta) + \dots \quad (6.4)$$

$$T_0 = T_{00}(\eta) + \zeta T_{01}(\eta) + \zeta^2 T_{02}(\eta) + \zeta^3 T_{03}(\eta) + \dots \quad (6.5)$$

where  $W_{00}(\eta)$  and  $T_{00}(\eta)$  represent the planar values of the velocity and temperature profiles respectively, and  $W_{01}(\eta)$  and  $T_{01}(\eta)$  etc. correspond to the perturbations to the basic flow caused through curvature.

To leading order, equation (4.15) reduces to

$$\frac{d}{d\eta} \left\{ \frac{W_{00} \varphi_{0\eta} - W_{00\eta} \varphi_0}{T_{00} \left[ 1 + \frac{n^2}{\alpha^2} \right] - M_\infty^2 W_{00}^2} \right\} = 0 \quad (6.6)$$

$$\text{i.e. } W_{00} \varphi_{0\eta} - W_{00\eta} \varphi_0 = k_0 \left\{ T_{00} \left[ 1 + \frac{n^2}{\alpha^2} \right] - M_\infty^2 W_{00}^2 \right\}, \quad (6.7)$$

where  $k_0$  is a constant. However we require that  $\varphi_0(\eta=0) = 0$ , whilst  $\varphi_0$  is restricted not to grow exponentially as  $\eta \rightarrow \infty$ . Consequently we must have that

$$k_0 = 0, \quad (6.8)$$

and hence

$$\varphi_0 = A_0 W_{00}(\eta), \quad (6.9)$$

where  $A_0$  is an arbitrary constant (i.e. the unknown amplitude of the eigensolution).

Equation (6.6) is not a uniformly valid approximation to (4.15), for all  $\eta$ ; specifically a breakdown occurs when  $\eta = O(\zeta^{-1})$ . We define

$$\hat{\eta} = 1 + \zeta \eta = O(1), \quad (6.10)$$

(i.e.  $\hat{\eta}$  represents a scale comparable to the radius of the cone), and on this scale we expand  $\varphi$  as follows

$$\varphi = \hat{\phi}_0(\hat{\eta}) + \zeta \hat{\phi}_1(\hat{\eta}) + \dots \quad (6.11)$$

To leading order equation (4.15) reduces to

$$\frac{d}{d\hat{\eta}} \left\{ \frac{\hat{\phi}_0 \hat{\eta} + \frac{1}{\hat{\eta}} \hat{\phi}_0}{\left[1 + \frac{n^2}{\alpha^2 \hat{\eta}^2}\right] - M_\infty^2} \right\} = \alpha^2 \hat{\phi}_0 \quad (6.12)$$

The solution to this, which matches on to (6.9) as  $\hat{\eta} \rightarrow 1$  is

$$\hat{\phi}_0 = \frac{A_0 K_n' [i \alpha (M_\infty^2 - 1)^{\frac{1}{2}} \hat{\eta}]}{K_n' [i \alpha (M_\infty^2 - 1)^{\frac{1}{2}}]} \quad (6.13)$$

where  $K_n(z_1)$  is the Bessel function of order  $n$ , argument  $z_1$  (the  $K_n(z_1)$  solution is chosen in preference to the  $\text{Im}(z_1)$  solution in order that disturbances are propagated along characteristics in the downstream direction - see Ward 1955, Klauwick et al 1984, Duck and Hall 1989a,b).

Returning now to the  $\eta = O(1)$  layer, the  $O(\zeta)$  correction to  $\varphi$  is given by

$$\frac{d}{d\eta} \left\{ \frac{W_{01} \varphi_{0\eta} - c_1 \varphi_{0\eta} + W_{00} \varphi_{1\eta} + W_{00} \varphi_0 - W_{00\eta} \varphi_1 - W_{01\eta} \varphi_0}{T_{00} \left[1 + \frac{n^2}{\alpha^2}\right] - M_\infty^2 W_{00}^2} \right\} = 0, \quad (6.14)$$

and so integrating this equation once we obtain

$$\begin{aligned} & W_{01} \varphi_{0\eta} - c_1 \varphi_{0\eta} + W_{00} \varphi_{1\eta} + W_{00} \varphi_0 - W_{00\eta} \varphi_1 - W_{01\eta} \varphi_0 \\ & = k_1 \left\{ T_{00} \left[1 + \frac{n^2}{\alpha^2}\right] - M_\infty^2 W_{00}^2 \right\}, \end{aligned} \quad (6.15)$$

where  $k_1$  is an arbitrary constant.  $\varphi_1$  must not be exponentially large as  $\eta \rightarrow \infty$ , and consequently we must have

$$\varphi|_{\eta \rightarrow \infty} + A_0 = k_1 \left\{ 1 - M_\infty^2 + \frac{n^2}{\alpha^2} \right\}, \quad (6.16)$$

together with

$$-c_1 A_0 W_{00\eta}(\eta=0) = k_1 T_{00}(0) \left[ 1 + \frac{n^2}{\alpha^2} \right] \quad (6.17)$$

However in order to match correctly with (6.13)

$$\begin{aligned} \varphi|_{\eta \rightarrow \infty} &= \hat{\Phi}_{0\hat{\eta}}|_{\hat{\eta}=1} = 1 \\ &= \frac{A_0 i\alpha (M_\infty^2 - 1)^{\frac{1}{2}} K_n'' [i\alpha (M_\infty^2 - 1)^{\frac{1}{2}}]}{K_n' [i\alpha (M_\infty^2 - 1)^{\frac{1}{2}}]} \end{aligned} \quad (6.18)$$

Eliminating  $k_1$ , we obtain the following result for  $c_1$

$$c_1 = \left\{ 1 + i\alpha (M_\infty^2 - 1)^{\frac{1}{2}} \frac{K_n'' [i\alpha (M_\infty^2 - 1)^{\frac{1}{2}}]}{K_n' [i\alpha (M_\infty^2 - 1)^{\frac{1}{2}}]} \right\} \quad (6.19)$$

$$\left\{ \frac{T_{00}(\eta=0) \left[ 1 + \frac{n^2}{\alpha^2} \right]}{W_{00\eta}(\eta=0) \left[ M_\infty^2 - 1 - \frac{n^2}{\alpha^2} \right]} \right\}$$

The asymptotic forms for this expression in the limit of large and small  $\alpha$  may be found readily. Firstly as  $\alpha \rightarrow \infty$  we have

$$c_1 \rightarrow \frac{-i\alpha T_{00}(\eta=0)}{W_{00\eta}(\eta=0)(M_\infty^2 - 1)^{\frac{1}{2}}} + O(\alpha^{-1}) \quad (6.20)$$

Secondly as  $\alpha \rightarrow 0$

$$c_1 \rightarrow \frac{n T_{00}(\eta=0)}{W_{00\eta}(\eta=0)} + O(\alpha^2) \quad \text{for } n \neq 1, \quad (6.21a)$$

$$c_1 \rightarrow \frac{n T_{00}(\eta=0)}{W_{00\eta}(\eta=0)} + O(\alpha^2 \log \alpha) \quad \text{for } n=1. \quad (6.21b)$$

In fact it is quite easy to show that as  $\alpha \rightarrow 0$ ,

$$\text{Im} \{c_1\} \rightarrow \frac{-\alpha^{2n} (M_\infty^2 - 1)^n T_{00}(0) 2^{2-2n}}{W_{00\eta}(0) [(n-1)!]^2} \quad (6.21c)$$

Equations (6.21) are precisely the (real) values found by Duck and Hall (1989b) for the downstream limit of a non-axisymmetric viscous mode

(taking into account the different scalings used in Duck and Hall's paper). Consequently we expect that as  $\zeta \rightarrow 0/\infty$ , on a scale smaller/larger than that of the cone radius, we expect this mode to become predominantly viscous in nature, and to be described by triple-deck theory.

Distributions of  $\text{Im}\{c_1\}$  with  $\alpha$  are shown in Fig. 12 for  $n = 1, 2, 3$  (with (6.20) also shown). Unfortunately (perhaps) it is seen that  $\text{Im}\{c_1\} < 0$  for all  $\alpha$  (confirmed by (6.20)). From (6.21) we also have that  $\text{Im}\{c_1\} = O(\zeta)$  as  $\zeta \rightarrow 0$ . Unfortunately, also, the  $O(\zeta^2)$  and higher correction to this mode would require a large amount of algebra. However we are able to make progress, in particular obtain an estimate for  $\text{Im}\{c(\alpha = 0)\}$  by considering instead the limit as  $\zeta \rightarrow 0$  of equation (A.2), pertinent to the  $\alpha \rightarrow 0$  case. (With  $\alpha = o(\zeta)$  we consider this aspect in the following subsection).

Finally, for this subsection, note that the  $\zeta \rightarrow \infty$  results may be simply inferred from these  $\zeta \rightarrow 0$  results, simply by replacing the small parameter ' $\zeta$ ' in the various expansions by the small parameter ' $1/\lambda\zeta$ '. More subtle differences between the  $\zeta \ll 1$  and  $\zeta \gg 1$  solutions only appear at higher orders.

### 6.2 $\alpha = 0, \zeta \rightarrow 0$ (or $\zeta \rightarrow \infty$ )

The system (A.2) turns out to be rather easier to analyse as  $\zeta \rightarrow 0$  than does the corresponding finite  $\alpha$  ( $= \alpha\zeta^{-1}$ ) problem. We again utilise expansions (6.2) - (6.5) (although see (6.48) for the  $\varphi$  expansion).

To leading order, we have for  $\eta = O(1)$  that

$$\varphi_0 = A_0 W_{00}(\eta), \quad (6.22)$$

where  $A_0$  is some (arbitrary) amplitude parameter.

At the next order we have the following system

$$\begin{aligned} W_{00} \varphi_{1\eta} - A_0 W_{00\eta} c_1 + A_0 W_{00}^2 \\ - W_{00\eta} \varphi_1 + A_0 W_{01} W_{00\eta} - A_0 W_{01\eta} W_{00} = k_1 T_{00}, \end{aligned} \quad (6.23)$$

where  $k_1$  is a constant, and we have utilised (6.22). Setting  $\eta = 0$  in (6.23), assuming  $\varphi_1|_{\eta=0} = 0$ , then

$$-A_0 c_1 w_{00\eta}(\eta=0) = k_1 T_{00}(\eta=0). \quad (6.24)$$

The boundary conditions as  $\eta \rightarrow \infty$  must be compatible with (A.3), together with (6.22). Defining

$$\bar{r} = 1 + \eta/\zeta = O(1), \quad (6.25)$$

then we must have an outer solution of the form

$$\varphi_0^{\text{out}} = \hat{A} \bar{r}^{-n-1}, \quad (6.26a)$$

$$\text{where } \hat{A} = A_0 + \zeta \hat{A}_1 + \dots, \quad (6.26b)$$

and so we must also have

$$\varphi_1 \eta \Big|_{\eta \rightarrow \infty} = \varphi_0^{\text{out}} \Big|_{\bar{r} = 1} = -(n+1)A_0. \quad (6.27)$$

Substituting this into (6.23) yields

$$c_1 = \frac{n T_{00}(\eta=0)}{w_{00\eta}(\eta=0)}, \quad (6.28)$$

in accord with (6.2i). In order to estimate complex values of  $c$  we must proceed to higher orders in  $\zeta$ .

At the next order in  $\zeta$  we obtain the following equation governing  $\varphi_2$ :

$$\begin{aligned} & w_{00} \varphi_{2\eta} + 2\lambda w_{00} \varphi_{0\eta} + 2\eta w_{00} \varphi_{1\eta} + w_{02} \varphi_{0\eta} \\ & - w_{02\eta} \varphi_0 + w_{01} \varphi_{1\eta} + \eta^2 w_{00} \varphi_{0\eta} - c_1 \varphi_{1\eta} \\ & + 2w_{01} \eta \varphi_{0\eta} + w_{01} \varphi_0 - w_{01\eta} \varphi_1 - 2\eta w_{01\eta} \varphi_0 \\ & - 2\eta c_1 \varphi_{0\eta} - c_2 \varphi_{0\eta} + w_{00} \varphi_1 + \eta w_{00} \varphi_0 \\ & - c_1 \varphi_0 - w_{00\eta} \varphi_2 - 2\lambda w_{00\eta} \varphi_0 - 2\eta \varphi_1 w_{00\eta} \\ & - \eta^2 w_{00\eta} \varphi_0 = k_2 T_{00} + n^2 T_{00} \int_0^\eta \frac{\varphi_0 w_{00}}{T_{00}} d\eta \\ & + k_1 T_{01}. \end{aligned} \quad (6.29)$$

We shall defer any consideration of this equation, and move to the next order of  $\zeta$ , which yields

$$\begin{aligned}
& W_{00} \varphi_{3\eta} + 2 \lambda W_{00} \varphi_{1\eta} + 2 \eta W_{00} \varphi_{2\eta} + 2 \lambda \eta W_{00} \varphi_{0\eta} \\
& + \eta^2 W_{00} \varphi_{1\eta} - c_1 \varphi_{2\eta} - 2\lambda c_1 \varphi_{0\eta} - 2\eta c_1 \varphi_{1\eta} \\
& - \eta^2 c_1 \varphi_{0\eta} - c_2 \varphi_{1\eta} - 2\eta c_2 \varphi_{0\eta} - c_3 \varphi_{0\eta} \\
& + W_{00} \varphi_2 + \lambda W_{00} \varphi_0 + \eta W_{00} \varphi_1 - c_1 \varphi_1 \\
& - c_1 \eta \varphi_0 - c_2 \varphi_0 - W_{00\eta} \varphi_3 - 2 \lambda W_{00\eta} \varphi_1 \\
& - \eta^2 W_{01\eta} \varphi_0 - 2\eta \varphi_2 W_{00\eta} - \eta^2 W_{00\eta} \varphi_1 \\
& + W_{01} \varphi_{2\eta} + 2\lambda W_{01} \varphi_{0\eta} + 2\eta W_{01} \varphi_{1\eta} \\
& + \eta^2 W_{01} \varphi_{0\eta} + W_{02} \varphi_{1\eta} + 2\eta W_{02} \varphi_{0\eta} \\
& + W_{03} \varphi_{0\eta} + W_{01} \varphi_1 + W_{01} \eta \varphi_0 + W_{02} \varphi_0 \\
& W_{03\eta} \varphi_0 - 2\eta W_{02\eta} \varphi_0 - 2\lambda W_{01\eta} \varphi_0 \\
& - 2\lambda \eta W_{00\eta} \varphi_0 - W_{02\eta} \varphi_1 - 2\eta W_{01\eta} \varphi_1 \\
& - W_{01\eta} \varphi_2 = k_2 T_{01} + k_1 T_{02} + k_3 T_{00} \\
& + n^2 T_{00} \int_0^\eta \frac{[\varphi_1 T_{00} - \varphi_0 T_{01}] W_{00} - c_1 T_{00} \varphi_0 + W_{01} \varphi_0 T_{00}}{T_{00}^2} d\eta \\
& + n^2 T_{01} \int_0^\eta \frac{\varphi_0 W_{00} d\eta}{T_{00}} . \tag{6.30}
\end{aligned}$$

Our main goal here is now to determine the leading order imaginary component of the complex wavespeed  $c$  (we do, of course, already know the leading order real term). Now since the above equations just contain real coefficients, any imaginaries must, of necessity, only arise at a critical point, where,  $\dot{c} = W_{00}$ . Since  $c = O(\zeta)$ , this must occur when  $\eta = O(\zeta)$ . We therefore consider a thin layer relative to the  $\eta = O(1)$  scale, namely

$$\eta = \eta/\zeta = O(1) . \tag{6.31}$$

On this scale, the expansion for  $\varphi$  is expected to develop as

$$\varphi = \zeta \Phi_0(\eta) + \zeta^2 \Phi_1(\eta) + \zeta^3 \Phi_2(\eta) + \dots , \tag{6.32}$$

where the  $\Phi_i$  are expected to be normalised in such a way as to be generally  $O(1)$  quantities.

It is easy to show that

$$\Phi_0(\eta) = A_0 W_{00\eta}(\eta=0) \eta \quad (6.33)$$

(where  $A_0$  was introduced in (6.22)), and also

$$\Phi_1(\eta) = A_1 W_{00\eta}(\eta=0) \tilde{\eta}, \quad (6.34)$$

where  $A_1$  is a constant, linearly related to  $A_0$ , and we have used the property that  $W_{00\eta}(\eta=0) = 0$ .

After some algebra, the equation for  $\Phi_2(\tilde{\eta})$  may be written

$$\begin{aligned} & [W_{00\eta}(0) \tilde{\eta} - c_1] \Phi_{2\tilde{\eta}} - W_{00\eta}(0) \Phi_2 \\ &= \hat{k}_2 + 3\tilde{\eta} c_1 A_0 W_{00\eta}(0) + \frac{1}{3} \tilde{\eta}^3 A_0 W_{00\eta\eta\eta}(0) W_{00\eta}(0) \\ &\quad - [W_{00\eta}(0)]^2 A_0 \tilde{\eta}^2 \\ &\quad - \frac{W_{00\eta}(0) T_{00\eta\eta}(0) c_1 A_0 \tilde{\eta}^2}{2 T_{00}(0)}, \end{aligned} \quad (6.35)$$

where here  $\hat{k}_2$  is an (arbitrary) constant.

If we take (as we are quite at liberty to do)  $A_0$  and  $\hat{k}_2$  to be real constants (this is not essential for our arguments, but simplifies the following argument), then we now consider just  $\Phi_2^i$  (where here and elsewhere a superscript  $i$  denotes an imaginary component). This quantity is triggered by the well known  $+i\pi$  jump in the logarithm (Mack, 1984 for example) across the critical layer. Specifically, here, this is caused by the  $\tilde{\eta}$  dependancy on the right-hand-side of equation (6.35) ( $\hat{k}_2$  plays no role in this). If (6.35) is written symbolically as

$$[W_{00\eta}(0) \tilde{\eta} - c_1] \Phi_{2\tilde{\eta}} - W_{00\eta}(0) \Phi_2 = \hat{R}, \quad (6.36)$$

then

$$\Phi_2 = [W_{00\eta}(0) \tilde{\eta} - c_1] \int_0^{\tilde{\eta}} \frac{\hat{R} d\tilde{\eta}}{[W_{00\eta}(0) \tilde{\eta} - c_1]^2}. \quad (6.37)$$

Evaluating this integral, taking just the imaginaries together with the limit as  $\eta \rightarrow \infty$  yields

$$\begin{aligned} \phi_2^i &\sim \pi A_0 [w_{00\eta}(0) \eta - c_1] c_1 \left\{ \frac{1}{w_{00\eta}(0)} + c_1 \frac{w_{00\eta\eta\eta}(0)}{[w_{00\eta}(0)]^3} \right. \\ &\quad \left. - \frac{T_{00\eta\eta}(0) c_1}{T_{00}(0) [w_{00\eta}(0)]^2} \right\} \\ &= B^i [w_{00\eta}(0) \eta - c_1] , \end{aligned} \quad (6.38)$$

$$\begin{aligned} \text{where } B^i &= \pi A_0 c_1 \left\{ \frac{1}{w_{00\eta}(0)} + c_1 \frac{w_{00\eta\eta\eta}(0)}{[w_{00\eta}(0)]^3} \right. \\ &\quad \left. - \frac{T_{00\eta\eta}(0) c_1}{T_{00}(0) [w_{00\eta}(0)]^2} \right\} . \end{aligned} \quad (6.39)$$

Equation (6.38) then provides the lower boundary conditions for the system (6.29) and (6.30).

Since (6.29) contains just real coefficients (and taking  $c_2$  to be real, an assumption that may be justified a posteriori), then we must have

$$\phi_2^i = B^i w_{00}(\eta) , \quad (6.40)$$

where  $B^i$  is defined in (6.39).

If we take the imaginary part of (6.30) and allow  $\eta \rightarrow \infty$ , then

$$\phi_{3\eta}^i \Big|_{\eta \rightarrow \infty} + \phi_2^i \Big|_{\eta \rightarrow \infty} = k_3^i . \quad (6.41)$$

However we require (on account of (A.3)) that

$$\begin{aligned} \phi_{3\eta}^i \Big|_{\eta \rightarrow \infty} &\sim - (n+1) \phi_2^i \Big|_{\eta \rightarrow \infty} \\ &\sim - (n+1) B^i . \end{aligned} \quad (6.41)$$

$$\text{and so} \quad k_3^i = - n B^i . \quad (6.42)$$

Setting  $\eta = 0$  in (6.30) yields

$$\begin{aligned} -c_1 \phi_{2\eta}^i \Big|_{\eta=0} - c_3^i A_0 w_{00\eta}(0) - w_{00\eta}(0) \phi_3^i \Big|_{\eta=0} \\ = - n B^i T_{00}(0) \end{aligned} \quad (6.43)$$

However from (6.38) we have

$$\varphi_{2\eta}^i \Big|_{\eta=0} = B^i W_{00\eta}(0) . \quad (6.44)$$

$$\varphi_3^i \Big|_{\eta=0} = c_1 B^i . \quad (6.45)$$

Consequently, (after substituting for  $c_1$ ),

$$c_3^i = n^2 \frac{T_{00}(0)^2 \pi}{[W_{00\eta}(0)]^2} \left\{ \frac{1}{W_{00\eta}(0)} + \frac{n T_{00}(0) W_{00\eta\eta}(0)}{[W_{00\eta}]^4} - \frac{T_{00\eta\eta}(0) n}{[W_{00\eta}(0)]^3} \right\} \quad (6.46)$$

Using the governing equations for the basic flow allows this expression to be simplified slightly, to

$$c_3^i = \frac{n^2 T_{00}(0)^2 \pi}{[W_{00\eta}(0)]^3} \left\{ 1 + 2\sigma M_\infty^2 (\gamma-1)n \right\} . \quad (6.47)$$

In fact the expansion for  $\varphi$  in (6.5) is not quite complete as it stands, since the analysis of the  $\eta = 0(1)$  layer above indicates the presence of logarithmic terms; specifically we require

$$\begin{aligned} \varphi = & \varphi_0(\eta) + \zeta \varphi_1(\eta) + \zeta^2 \varphi_2(\eta) + \zeta^3 \varphi_3(\eta) + \dots \\ & + \log \zeta \left[ \zeta^2 \varphi_{21}(\eta) + \zeta^3 \varphi_{31}(\eta) + \dots \right] , \end{aligned} \quad (6.48)$$

$$\text{where} \quad \varphi_{21}(\eta) = A_{21} W_{00}(\eta) , \quad (6.49)$$

with  $A_{21}$  a constant.

A comparison of the fully numerical computation of  $\text{Real} \{ c(\alpha=0) \}$ , with the asymptotic formula (6.28), as  $\zeta \rightarrow 0$  is shown in Fig. 13. The agreement is seen to be entirely satisfactory. Unfortunately the correlation between the computed  $\text{Im} \{ c(\alpha=0) \}$  and that obtained using (6.47) is much less satisfactory. However, this poor correlation is not unexpected for two reasons. Firstly accurate computations of  $\text{Im} \{ c \}$  in this limit become exceedingly difficult, as confirmed by the quite complex asymptotic structure detailed above, with both thin

( $\eta = 0$  ( $\zeta$ )) and thick ( $\eta = 0$  ( $1/\zeta$ )) lengthscales emerging.

Secondly the asymptotic form for  $\text{Im} \{ c_1 \}$  is achieved very slowly as  $\zeta \rightarrow 0$ , at least in one particular configuration, where, with  $n = 1$ , the imaginary wavespeed has a leading order coefficient of approximately  $3.898 \times 10^5 \zeta^3$ . A comparison between the numerical and asymptotic results is not shown in this case.

In the case of  $\zeta \rightarrow \infty$ , we may just replace the small parameter ' $\zeta$ ' in the above, by the small parameter ' $1/\lambda\zeta$ '. In the following subsection, we consider the behaviour of mode I, as  $\zeta \rightarrow 0$ .

### 6.3 $\zeta \rightarrow 0$ , $\alpha = 0(\zeta^{\frac{1}{2}})$

The numerical results presented in the previous section strongly suggest that for the most part, as  $\zeta \rightarrow 0$  mode I has features very similar to the planar case, for all values of  $n$ . However there is one important exception to this, namely the behaviour of the lower neutral point in this limit. The planar case has that  $c \rightarrow 1 - 1/M_\infty$  as  $\alpha \rightarrow 0$ , corresponding to the so-called "sonic" mode. However in the case of our numerical results, there is evidence of a shift in this neutral point, along the positive real axis, and the neutral point becomes (slightly) supersonic, with  $c < 1 - 1/M_\infty$ , as  $\zeta \rightarrow 0$ .

A (sensible) balancing of terms suggests that we might look for a solution of the form

$$\begin{aligned} c &= \hat{c}_0 + \hat{c}_1 + \dots \\ \varphi &= \varphi_0 + \zeta \varphi_1 + \dots \\ w_0 &= w_{00} + \zeta w_{01} + \dots \\ T_0 &= T_{00} + \zeta T_{01} + \dots \end{aligned} \quad (6.50)$$

with

$$\alpha = \zeta^{\frac{1}{2}} \hat{\alpha}, \quad \hat{\alpha} = 0(1). \quad (6.51)$$

To leading order, (4.15) yields

$$\frac{d}{d\eta} \left\{ \frac{(W_{00} - \hat{c}_0) \varphi_{0\eta} - W_{0\eta} \varphi_0}{\tau_0} \right\} = 0 \quad (6.52)$$

where

$$\tau_0 = T_{00} - M_\infty^2 (W_{00} - \hat{c}_0)^2. \quad (6.53)$$

The solution to (6.52) which satisfies the impermeability condition on  $\eta = 0$  is

$$\varphi_0 = \hat{K}_0 (W_{00} - \hat{c}_0) \int_0^\eta \frac{\tau_0}{(W_{00} - \hat{c}_0)^2} d\eta, \quad (6.53)$$

where  $\hat{K}_0$  is some arbitrary constant, and the integral is to be taken underneath the critical point.

Since we require that  $\varphi_0 \rightarrow \text{constant}$  as  $\eta \rightarrow \infty$  (in order to match with (4.18)) we must have that

$$\hat{c}_0 = 1 \pm 1/M_\infty. \quad (6.54)$$

in order that the integral (6.53) remains bounded as  $\eta \rightarrow \infty$ . Further, we take the negative sign to be consistent with the numerical results and our comments above; indeed, this is simply a repeat of the planar calculation (Lees and Lin 1946).

Curvature plays an important role at next order, namely  $O(\zeta)$ . The governing equation in this case is

$$\begin{aligned} \frac{d}{d\eta} \left\{ \frac{1}{\tau_0} \left[ (W_{00} - \hat{c}_0)(\varphi_{1\eta} + \varphi_0) - \hat{c}_1 \varphi_{0\eta} - W_{00\eta} \varphi_1 + W_{01} \varphi_{0\eta} - W_{01\eta} \varphi_0 \right] \right. \\ \left. \frac{1}{\tau_0^2} \left[ (W_{00} - \hat{c}_0) \varphi_{0\eta} - W_{00\eta} \varphi_0 \right] \left[ n^2 \frac{T_{00}}{\alpha^2} + T_{01} \right. \right. \\ \left. \left. + 2M_\infty^2 (W_{00} - \hat{c}_0) \hat{c}_1 - 2M_\infty^2 (W_{00} - \hat{c}_0) W_{01} \right] \right\} \\ = \frac{\alpha^2 (W_{00} - \hat{c}_0) \varphi_0}{\tau_{00}}. \quad (6.55) \end{aligned}$$

Consequently, using (6.53),

$$\begin{aligned}
& (W_{00} - \hat{c}_0) (\varphi_{1\eta} + \varphi_0) - \hat{c}_1 \varphi_{0\eta} - W_{00\eta} \varphi_1 - W_{01\eta} \varphi_0 \\
& \hat{K}_0 \left[ \frac{n^2 T_{00}}{\alpha^2} + T_{01} + 2M_\infty^2 (W_{00} - \hat{c}_0) c_1 - 2M_\infty^2 (W_{00} - \hat{c}_0) W_{01} \right] \\
& = \hat{K}_1 \tau_0 + \alpha^2 \tau_0 \int_0^\eta \frac{(W_{00} - \hat{c}_0) \varphi_0}{T_{00}} d\eta, \quad (6.56)
\end{aligned}$$

where  $\hat{K}_1$  is a constant.

In order to match correctly at the outer edge ( $\eta \rightarrow \infty$ ) with (4.18), we must have that

$$\varphi_{1\eta} \Big|_{\eta \rightarrow \infty} = \frac{\hat{\eta}_0 K_n''(\hat{\eta}_0) \hat{K}_0 I}{K_n'(\hat{\eta}_0) M_\infty}, \quad (6.57)$$

where

$$I = \int_0^\infty \frac{T_0}{(W_{00} - \hat{c}_0)^2} d\eta, \quad (6.58)$$

$$\text{and} \quad \hat{\eta}_0 = M_\infty^{\frac{1}{2}} \alpha (2\hat{c}_1)^{\frac{1}{2}} \quad (6.59)$$

Taking the  $O(1)$  terms of (6.56) as  $\eta \rightarrow \infty$  and using (6.57) yields the following non-linear dispersion relationship for  $\hat{c}_1$ :

$$\hat{\eta}_0 \frac{K_n''(\hat{\eta}_0)}{K_n'(\hat{\eta}_0)} + 1 = \frac{M_\infty^2}{T} \left[ \frac{n^2}{\alpha^2} + 2M_\infty \hat{c}_1 \right]. \quad (6.60)$$

The integral (6.58) was evaluated numerically, and for the conditions prevailing in all our numerical results it was found  $I \simeq -228.4 - 59.3i$ . Equation (6.60) was solved using Newton iteration, and results for  $\text{Real} \{ \hat{c}_1 \}$  and  $\text{Im} \{ \hat{c}_1 \}$  for various  $n$  are shown in Figs. 13a and 13b respectively.

Notice that as  $\hat{\alpha} \rightarrow \infty$ , (6.60) predicts that one family of solutions has the property that

$$\hat{c}_1 \rightarrow \frac{\hat{\alpha}^2 I^2}{2 M_\infty^5}. \quad (6.61)$$

which is in agreement with the  $\alpha \ll 1$  expansion for  $c$  for the planar case, namely

$$c = 1 - 1/M_\infty + \frac{\alpha^2}{2 M_\infty^5} + O(\alpha^4) . \quad (6.62)$$

Equation (6.61) is shown as an asymptotic on Figs. 14a and 14b. Note that the (real) family of  $\hat{c}_1$  which also exist may be found as an exact solution to (6.60), namely

$$\hat{c}_1 = - \frac{n^2}{2 M_\infty \alpha^2} , \quad (6.63)$$

although the importance of this mode is not thought to be great. The complex families of  $\hat{c}_1$ 's are seen to terminate at a finite value of  $\hat{\alpha}$ , corresponding to the (lower) neutral point of mode I. Notice that in all cases because  $\text{Real} \{ \hat{c}_1 \} < 0$  at the termination point, these modes correspond to supersonic neutral modes.

From the result shown in Fig. 14b, we are therefore able to offer an estimate for the position of the lower neutral point of mode I as  $\zeta \rightarrow 0$ . In particular, for the freestream conditions considered throughout this paper, for  $n = 0$  this position is given by  $\alpha \simeq 0.1 \zeta^{\frac{1}{2}}$ , for  $n = 1$  by  $\alpha \simeq 0.20 \zeta^{\frac{1}{2}}$ , and for  $n = 2$  by  $\alpha \simeq 0.295 \zeta^{\frac{1}{2}}$ . Comparing these asymptotic results with figure 4 in particular reveals a fair degree of agreement.

In the case of  $\zeta \gg 1$ , the above results may be easily transposed, by the replacement of ' $\zeta$ ' by ' $1/\lambda\zeta$ '; the corresponding positions for lower neutral point are then  $\alpha \simeq 0.1 (\lambda\zeta)^{-\frac{1}{2}}$  for  $n = 0$ ,  $\alpha \simeq 0.20 (\lambda\zeta)^{-\frac{1}{2}}$  for  $n = 1$ , and  $\alpha \simeq 0.295 (\lambda\zeta)^{-\frac{1}{2}}$  for  $n = 2$ . These results are seen to agree quite well with the  $\zeta = 75$  results shown in Fig. 11.

## 7. Conclusions

In this paper we have studied the supersonic boundary layer flow, and the inviscid stability thereof, over a sharp cone with adiabatic wall conditions. The basic flow is seen to evolve from one planar state, to a second, as predicted by the Mangler (1946) Transform.

The "triple generalised inflexion condition" is derived, this being the necessary condition for subsonic neutral modes, and is a (second) generalisation of the well known generalised inflexion condition.

Significantly, the numerical results point to the occurrence of a third mode of instability, not found in similar planar and (more recently) axisymmetric studies. An asymptotic study of this mode shows this mode to be linked to a viscous mode found by Duck and Hall (1989b), a study based on triple-deck-theory.

The "sonic" neutral mode is found to be altered by curvature (and in fact becomes a supersonic neutral mode as revealed by the asymptotic analysis valid as  $\zeta \rightarrow 0$  and  $\zeta \rightarrow \infty$ .)

Significantly, our results show that the so called second mode (mode II) is not always the most unstable, at least in the case of non-axisymmetric modes.

**Acknowledgements**

This research was supported by the National Aeronautics and Space Administration under NASA contract No. NAS1 - 18605 where one of the authors (PWD) was in residence at the Institute for Computer Applications in Science and Engineering (ICASE), NASA Langley Research Centre, Hampton, VA 23665. S.J.S. was in the receipt of a Northern Ireland Education Department studentship. A number of computations were carried out at the University of Manchester Computer Centre, with computer time provided under S.E.R.C. Grant No. GR/E/25702. The authors also wish to thank Dr. M.G. Macaraeg, of NASA Langley, for some stimulating discussions on this problem.

References

- Brown, W.B. 1962. Norair Report No NOR-62-15 Northrup Aircraft Inc., Hawthorne, LA.
- Duck, P.W. 1989. ICASE Report No. 89-19 (To appear in J. Fluid Mech.)
- Duck, P.W. 1990. To appear in Proc. ICASE/NASA Langley Workshop on Instability and Transition (Springer-Verlag).
- Duck, P.W. and Hall, P. 1989a. Quart. J. Mech. Appl. Maths 42, 115 (Also ICASE Report No. 88-10, 1988).
- Duck, P.W. and Hall, P. 1989b to appear in J. Fluid Mech. (also ICASE Report No. 88-42, 1988).
- Kluwick, A., Gittler, P. and Bodonyi, R.J. 1984. J. Fluid Mech. 140, 281.
- Lees, L. and Lin, C.C. 1946. NACA Tech. Note No. 1115.
- Mack, L.M. Space programs summary, no. 37-23, p297, JPL, Pasadena, CA.
- Mack, L.M. Space programs summary no. 37-26 vol. IV, p165, JPL Pasadena, CA.
- Mack, L.M. 1965a AGARDograph 27, part 1, 329.
- Mack, L.M. 1965b in "Methods in computational physics", (B. Alder, S. Fernbach and M. Rotenberg eds) vol 4, 247, Academic, N.Y.
- Mack, L.M. 1969 J.P.L. Pasadena, CA Document No. 900-277 Rev. A.
- Mack, L.M. 1984 AGARD Report No. 709, 3-1.
- Mack, L.M. 1987a in Proc. ICASE workshop on the stability of time dependent and spatially varying flows. Springer-Verlag.
- Mack, L.M. 1987b. AIAA Paper 87-1413.
- Mangler, K.W. 1946. Gt. Brit. Ministry of Air Production Volkernode Rept. and Trans. 55.
- Michalke, A., 1971. Z. Flugwiss. 19, 319.
- Reshotko, E. 1962. NASA Tech. Note D-1220.
- Stewartson, K. 1964. The theory of laminar boundary layers in compressible fluids. Oxford University Press.

Thompson, P.A. 1972. Compressible fluid dynamics, Mc.Graw Hill.

Ward, G.N. 1955. Linearised theory of high speed flows, Cambridge University Press.

### Appendix A The zero number limit

In the case of axisymmetric modes (and indeed of planar modes, as considered by Lees and Lin 1946, Mack 1965a, b, 1984, 1987 for example), as  $\alpha \rightarrow 0$ , the wavespeed  $c$  approaches the sonic limit, i.e.

$$c \rightarrow 1 \pm 1/M_\infty. \quad (\text{A.1})$$

In the case of non-axisymmetric modes, however, this is no longer the case. As clearly illustrated in the results, when  $n \neq 0$ ,  $c_i \not\rightarrow 0$  as  $\alpha \rightarrow 0$ . The explanation is as follows.

If we (simply) allow  $\alpha \rightarrow 0$  (assuming  $n \neq 0$ ), then (4.15) reduces to

$$\begin{aligned} \frac{d}{d\eta} \left\{ \frac{(w_0 - c) [1 + \lambda \zeta^2 + \zeta \eta] [(1 + \lambda \zeta^2 + \zeta \eta) \varphi_\eta + \zeta \varphi]}{T_0} \right. \\ \left. - \frac{w_{0\eta} [1 + \lambda \zeta^2 + \zeta \eta]^2 \varphi}{T_0} \right\} \\ = \frac{n^2 \zeta^2 \varphi}{T_0} (w_0 - c) \end{aligned} \quad (\text{A.2})$$

As  $\eta \rightarrow \infty$ , this system clearly admits solutions of the form

$$\varphi \sim \eta^{-n-1} \quad (\text{A.3})$$

(together with  $\varphi = 0$  on  $\eta = 0$ ), which is completely compatible with the outer solution, where  $\hat{\eta} = 0(1)$ , ( $\hat{\eta}$  defined by (4.19)) namely (4.18).

Equation (A.2) then represents a reduced problem as  $\alpha \rightarrow 0$ , and indeed a reduced form of the triply generalised inflexion point condition (4.28) exists in this limit, namely

$$\frac{d}{d\eta} \left\{ \frac{w_{0\eta} (1 + \lambda \zeta^2 + \zeta \eta)^2}{T_0} \right\} = 0 \quad (\text{A.4})$$

The system (A.2) - (A.3) was solved in a number of cases (in an identical manner to the  $\alpha = 0(1)$  eigenvalue system) and its correctness was confirmed. Notice, however, since the actual temporal growth rate is  $\alpha c_i$ , then this still reduces to zero as  $\alpha \rightarrow 0$ .

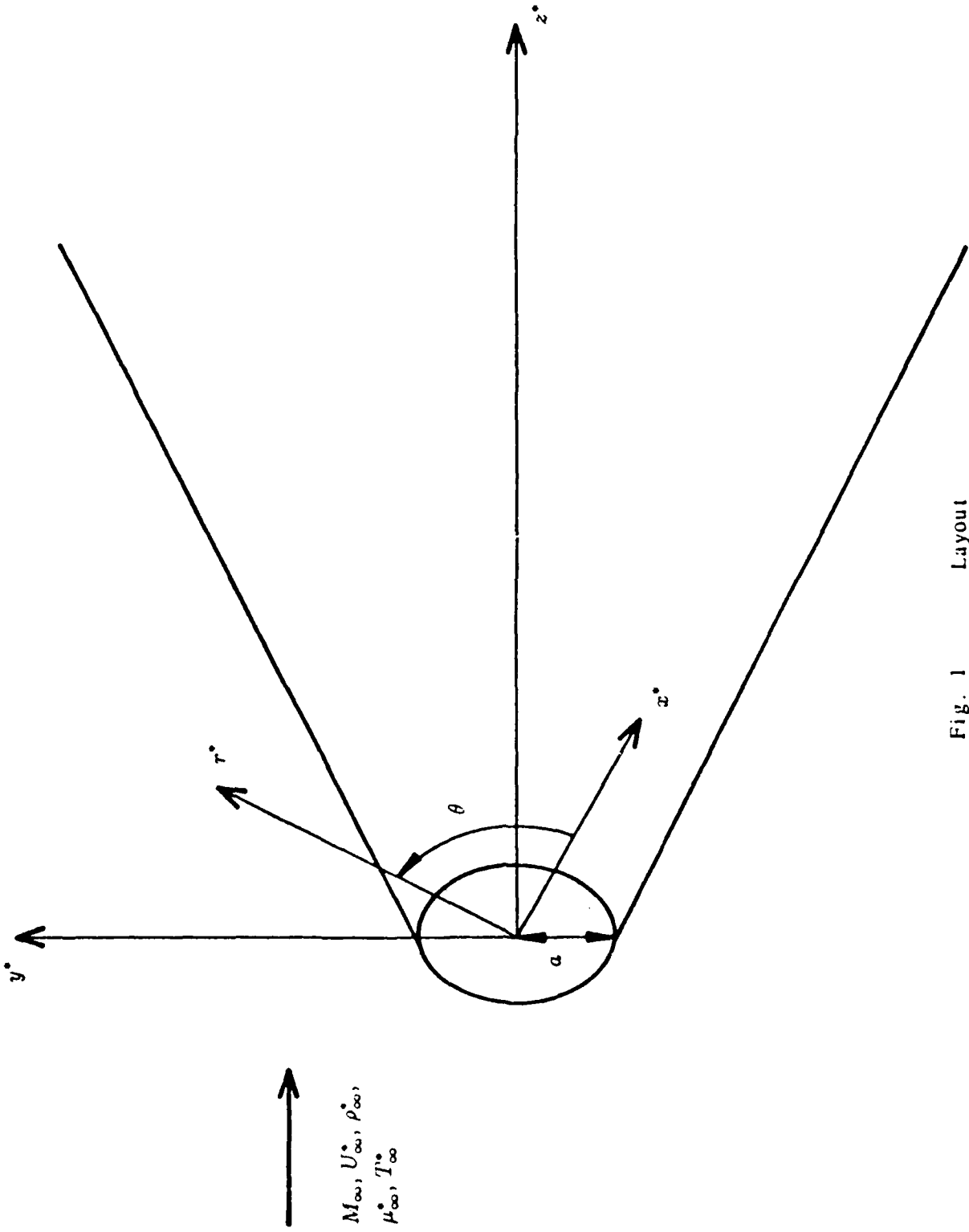


Fig. 1 Layout

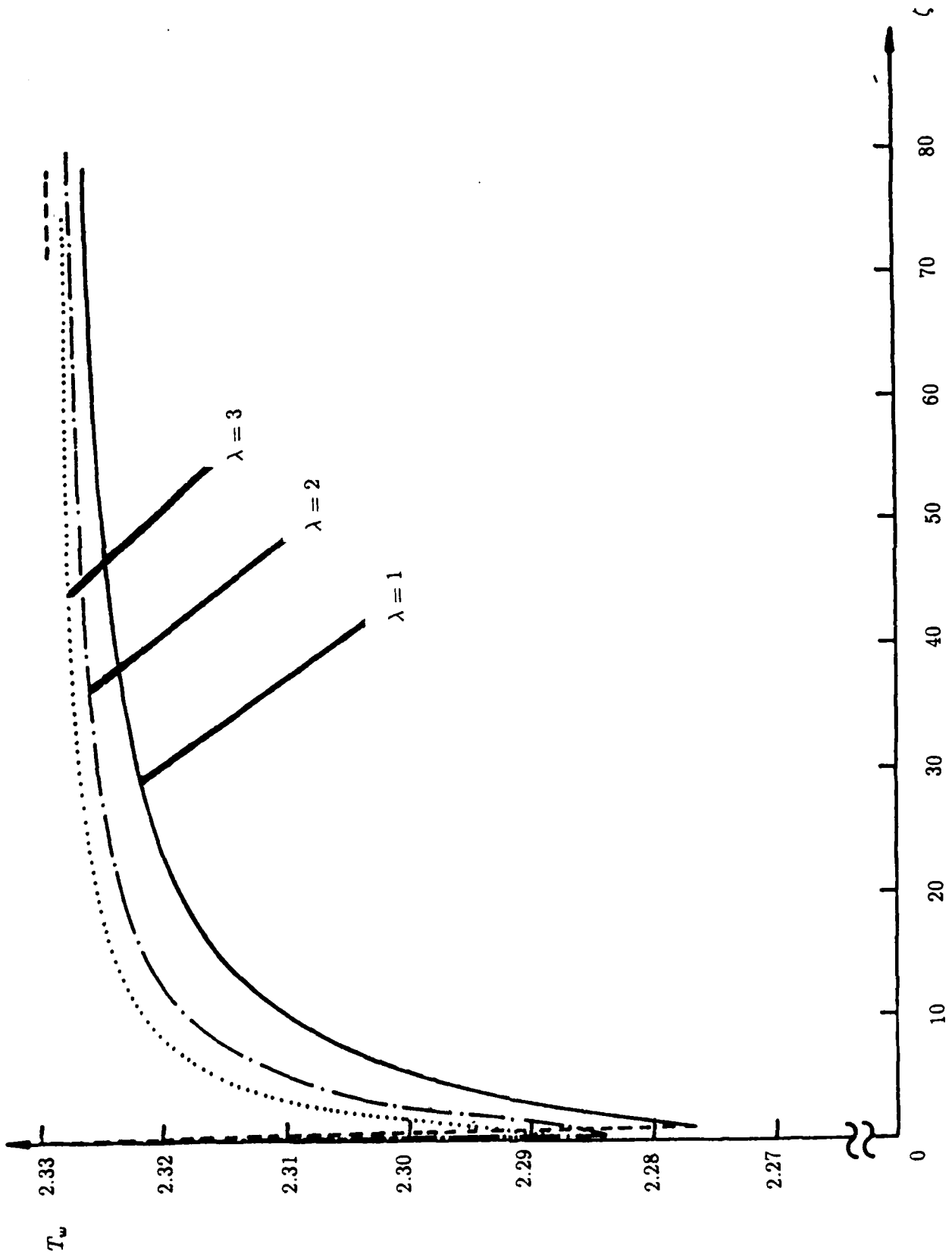


Fig.2a Axial wall temperature distributions,  $M_\infty = 2.8$

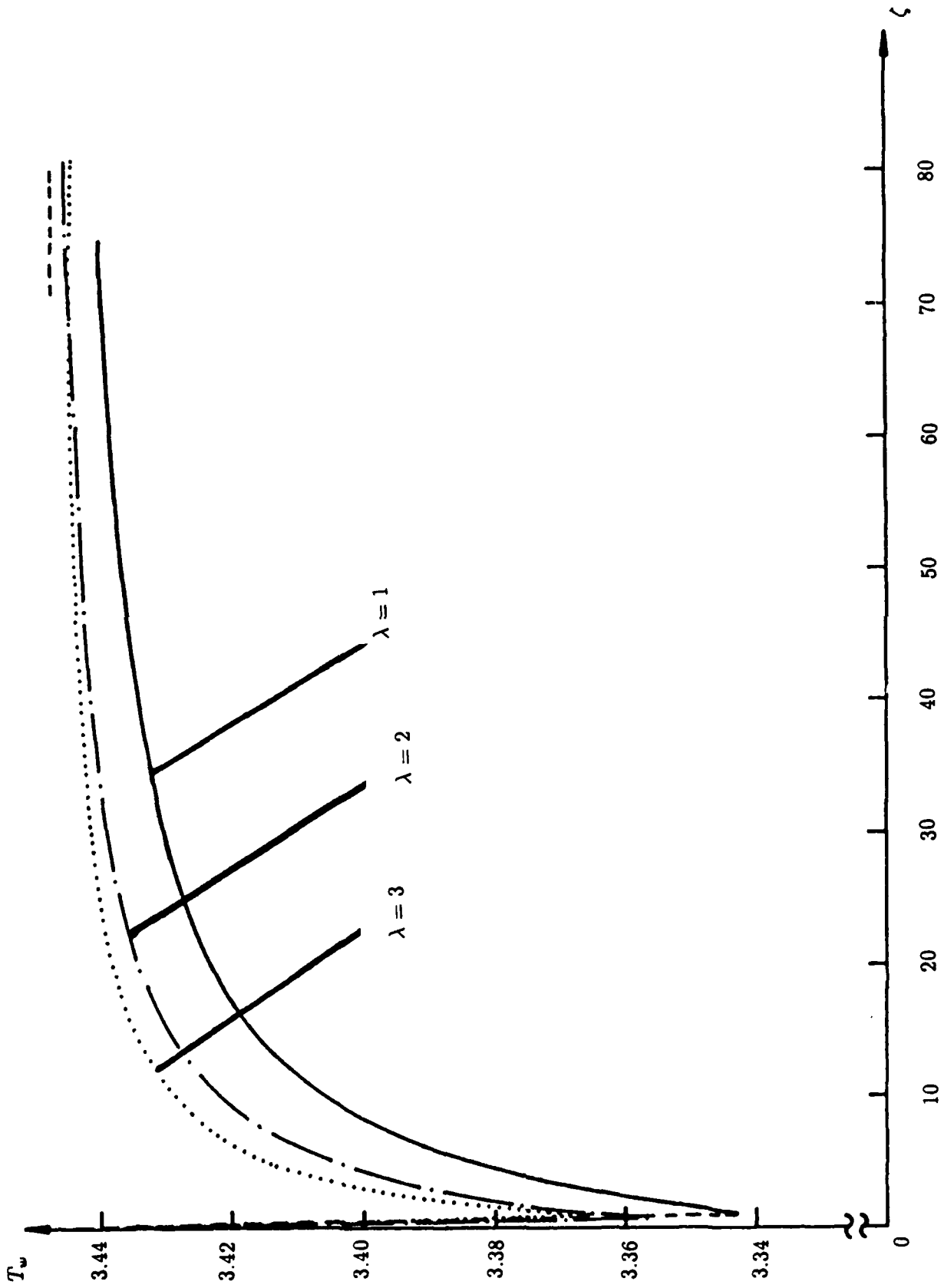


Fig. 2b Axial wall temperature distributions,  $M_\infty = 3.8$

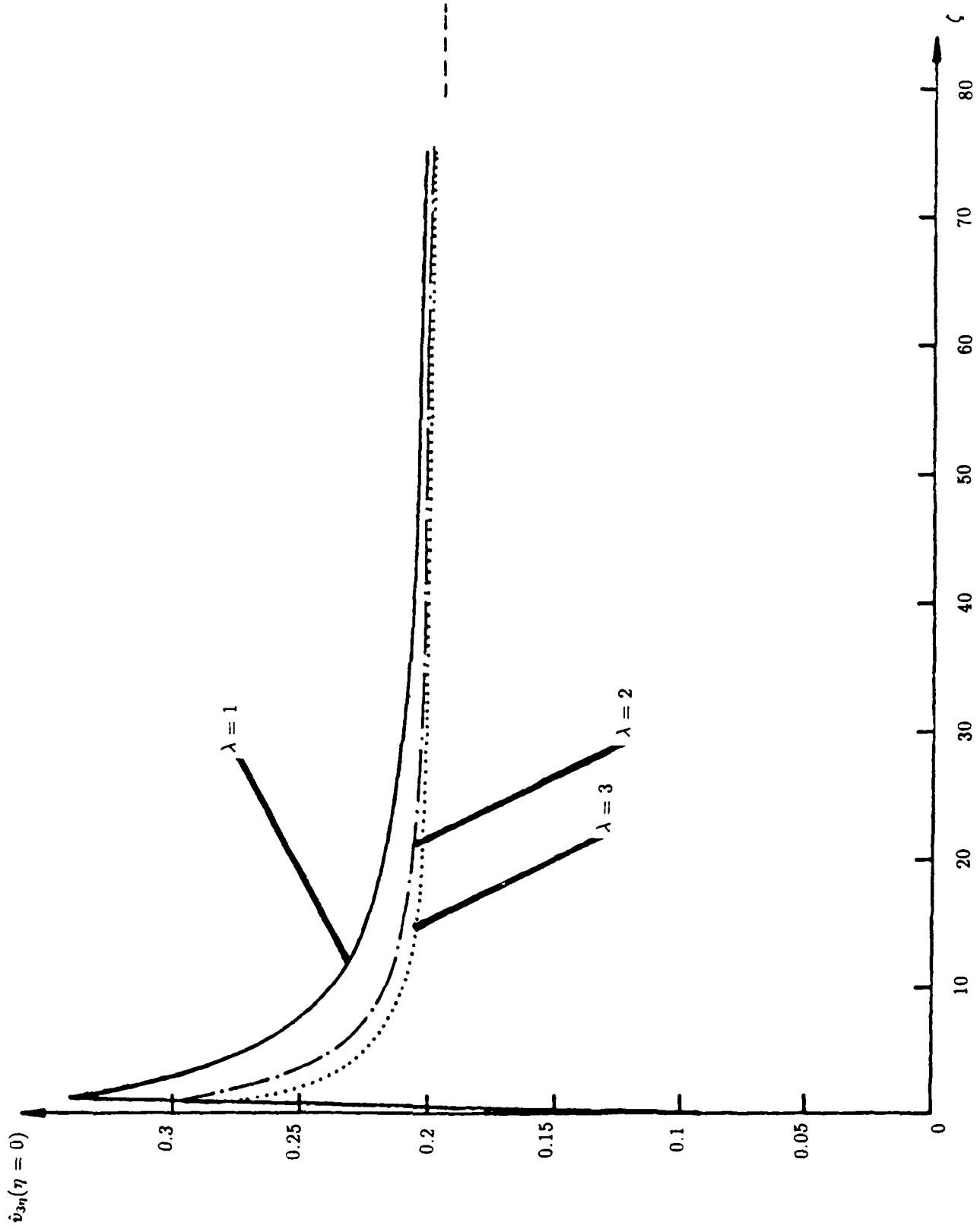


Fig. 3a Axial distributions of  $\dot{v}_{3\eta}|_{\eta=0}$ ,  $M_\infty = 2.8$

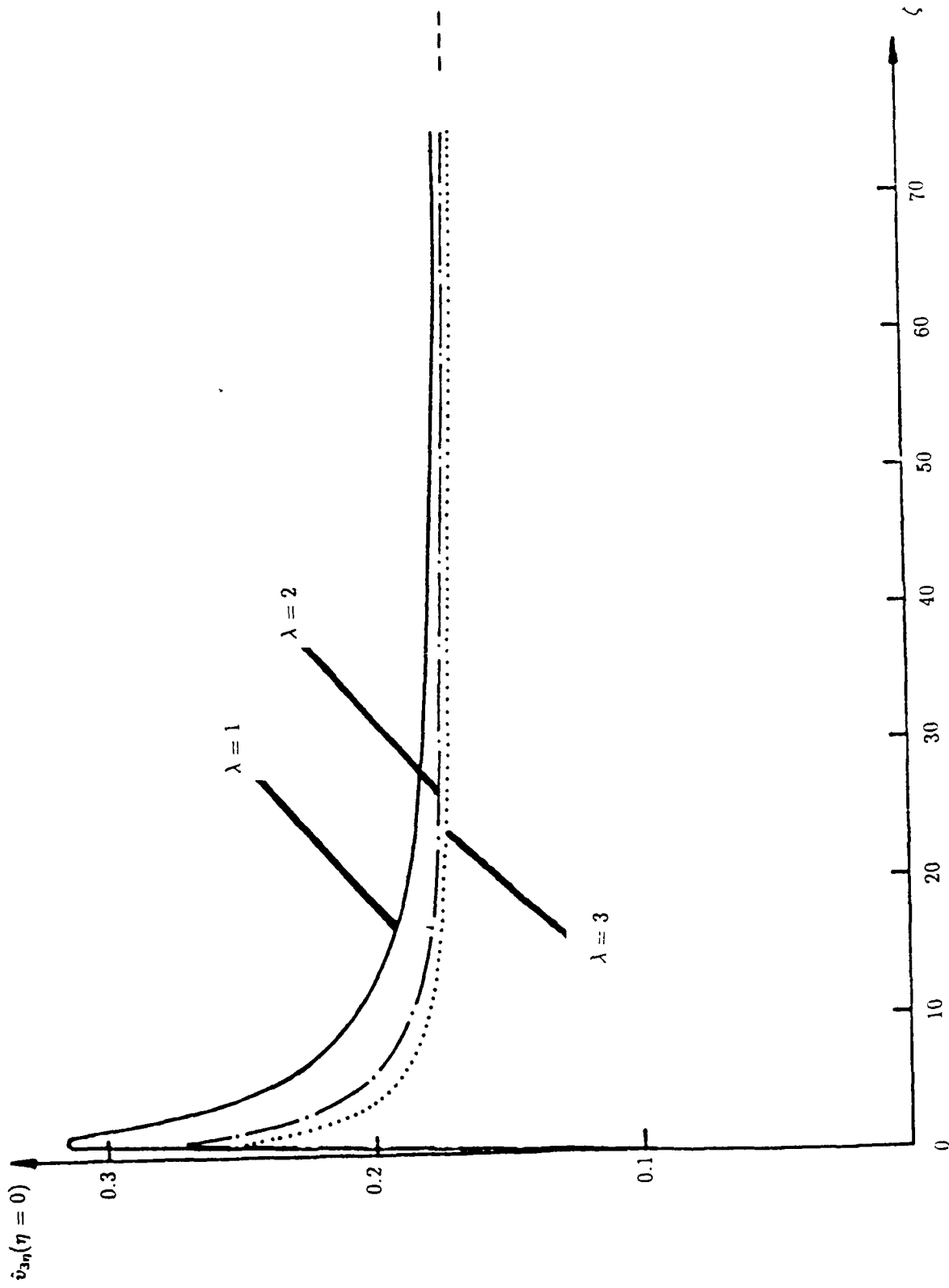


Fig. 3b Axial distributions of  $\hat{v}_{3\eta}(\eta=0)$ ,  $M_\infty = 3.8$

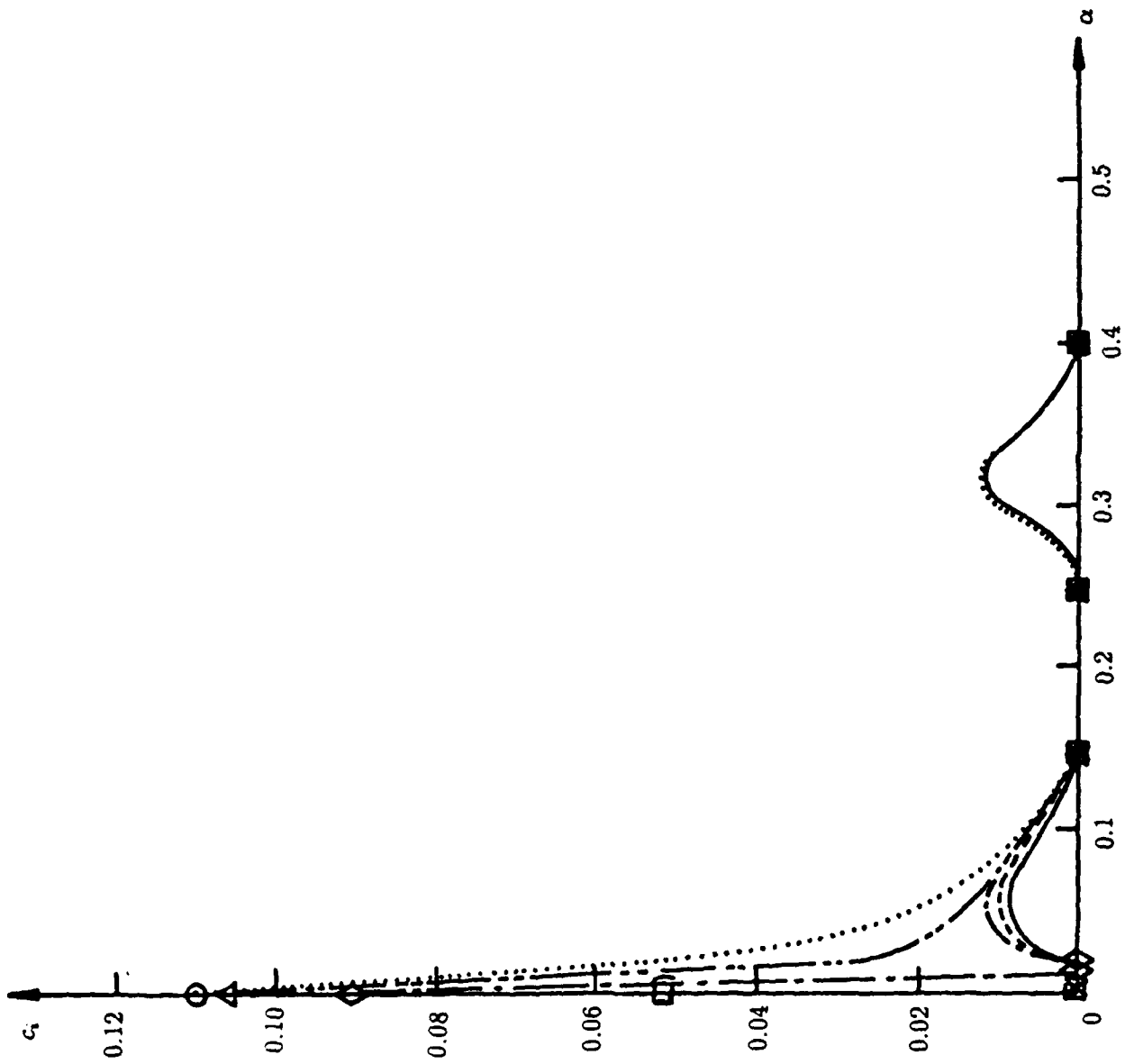


Fig.4 Distributions of  $c_j$  with  $\alpha$ ,  $M_w = 3.8$ ,  $\zeta = 0.01$

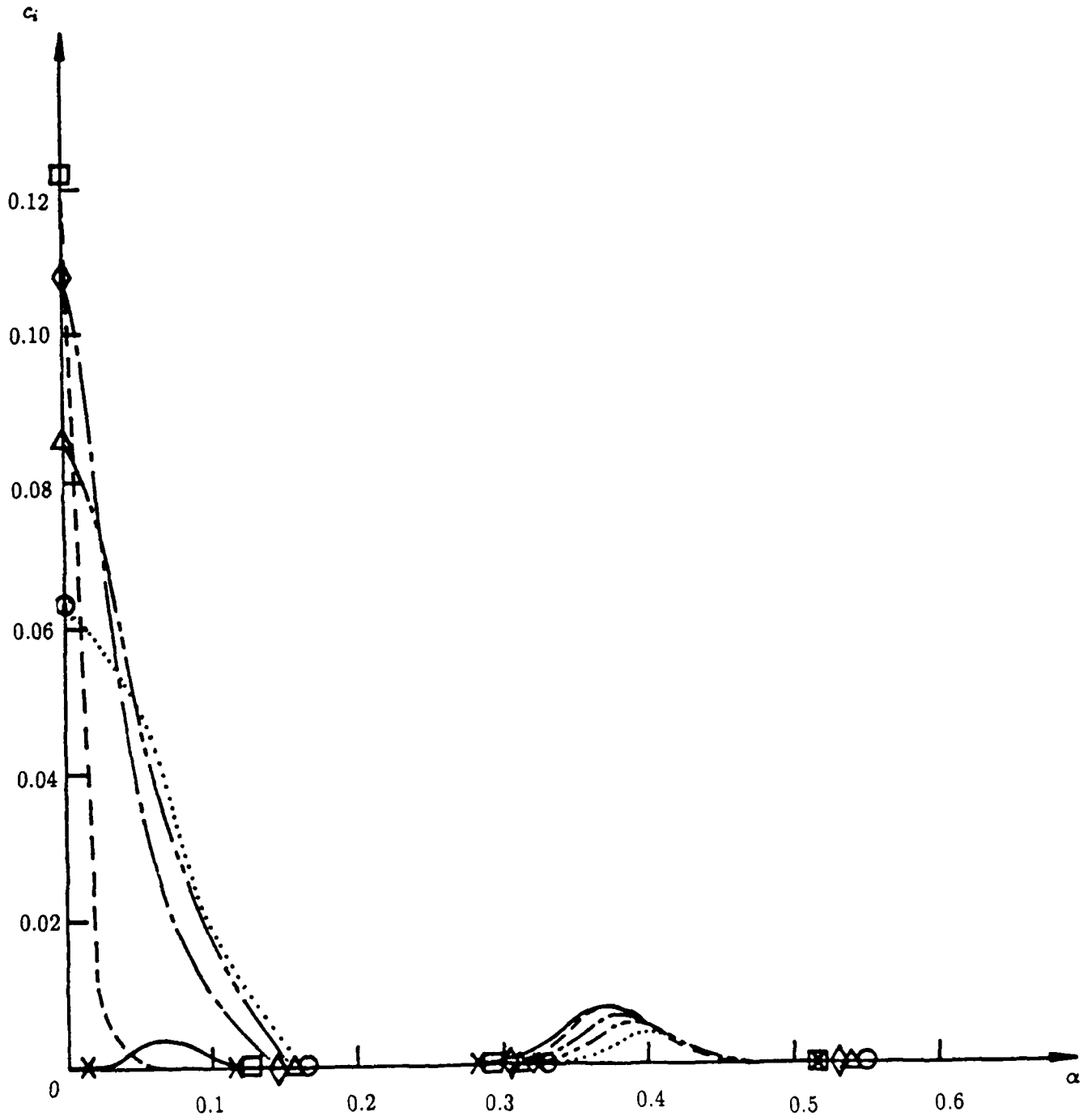


Fig.5 Distributions of  $c_i$  with  $\alpha$ ,  $M_\infty = 3.8$ ,  $\zeta = 0.05$

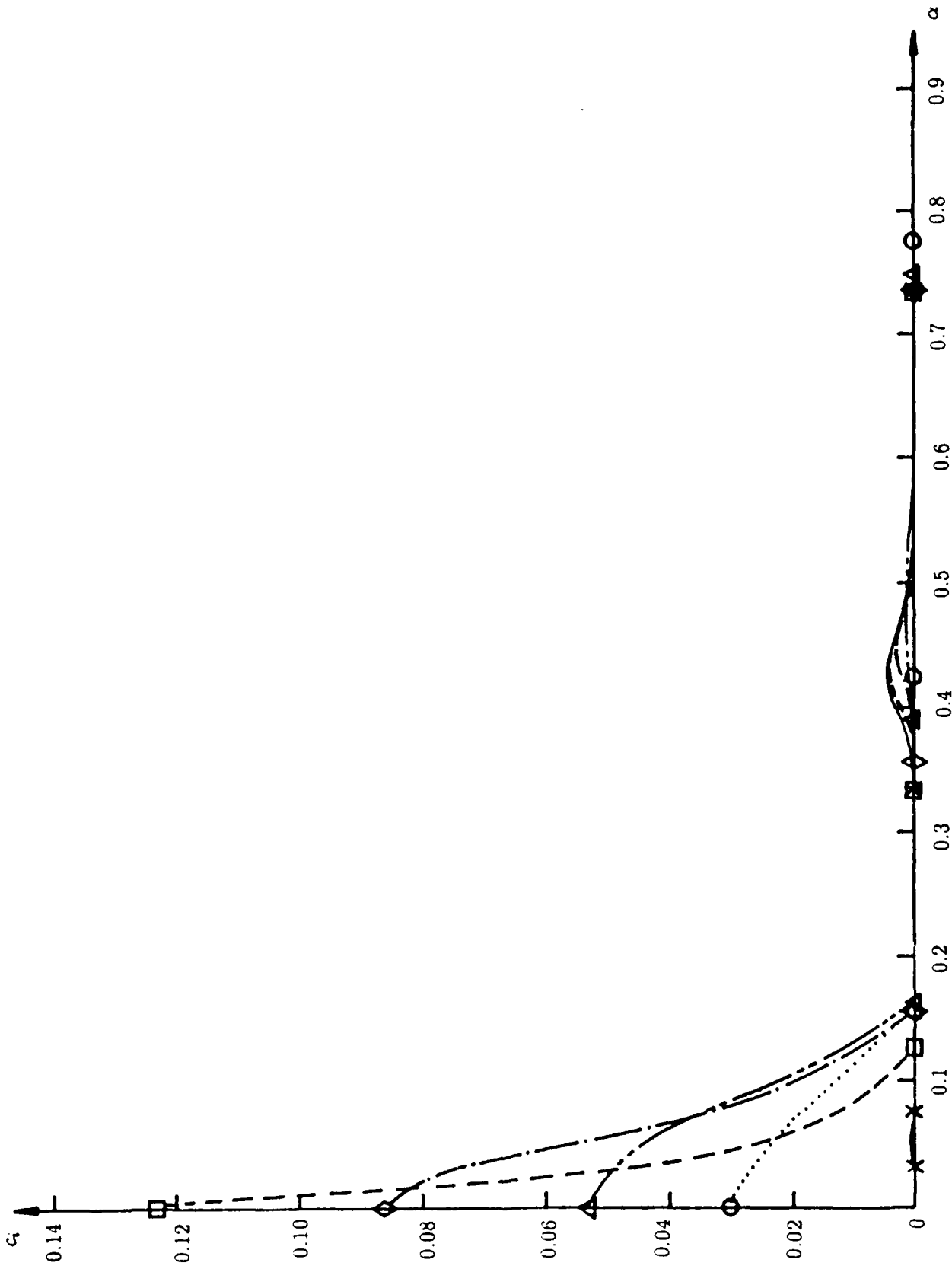


Fig.6 Distributions of  $c_i$  with  $\alpha$ ,  $M_\infty = 3.8$ ,  $\zeta = 0.10$

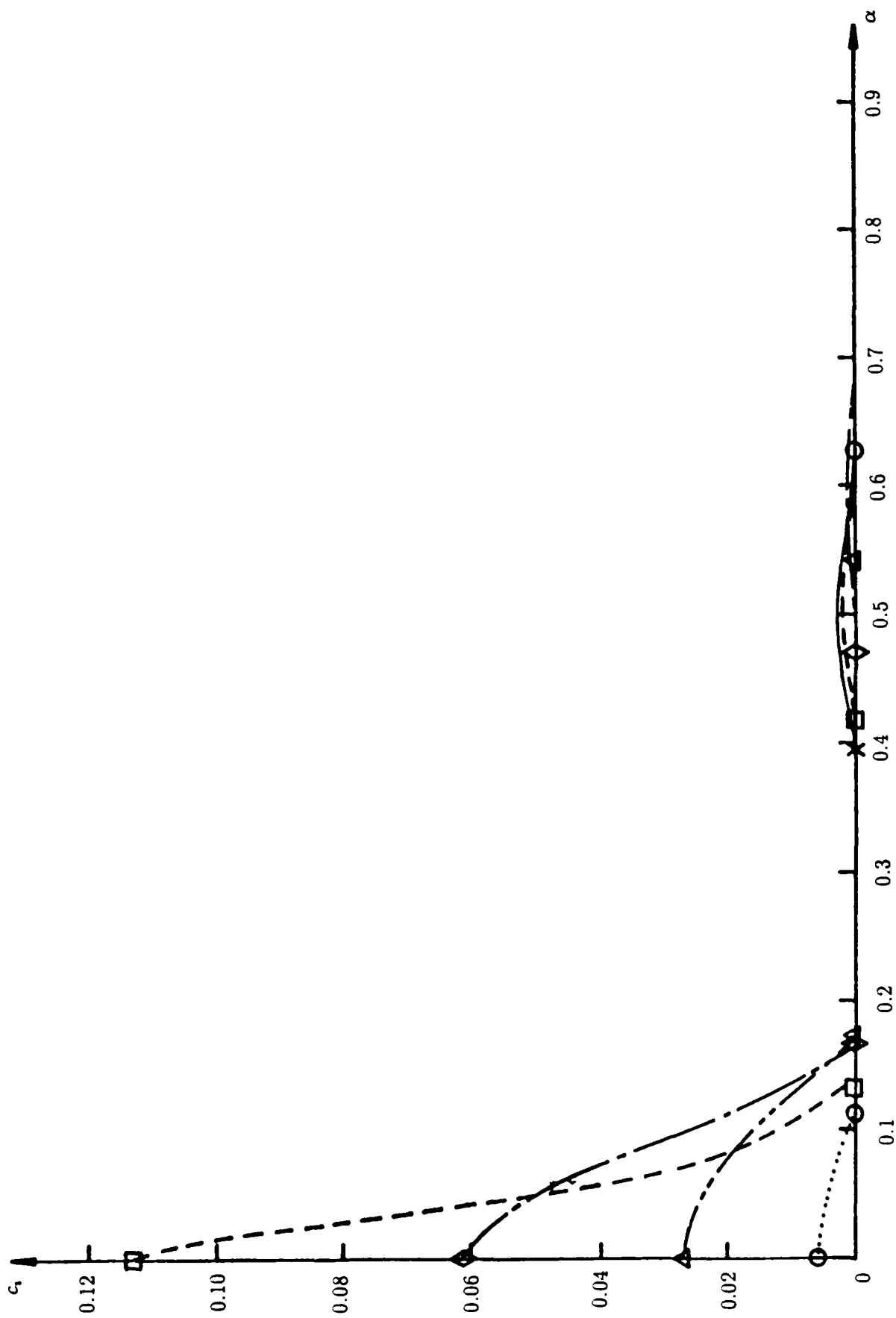


Fig.7a Distributions of  $c_j$  with  $\alpha$ .  $M_\infty = 3.8$ ,  $\zeta = 0.20$

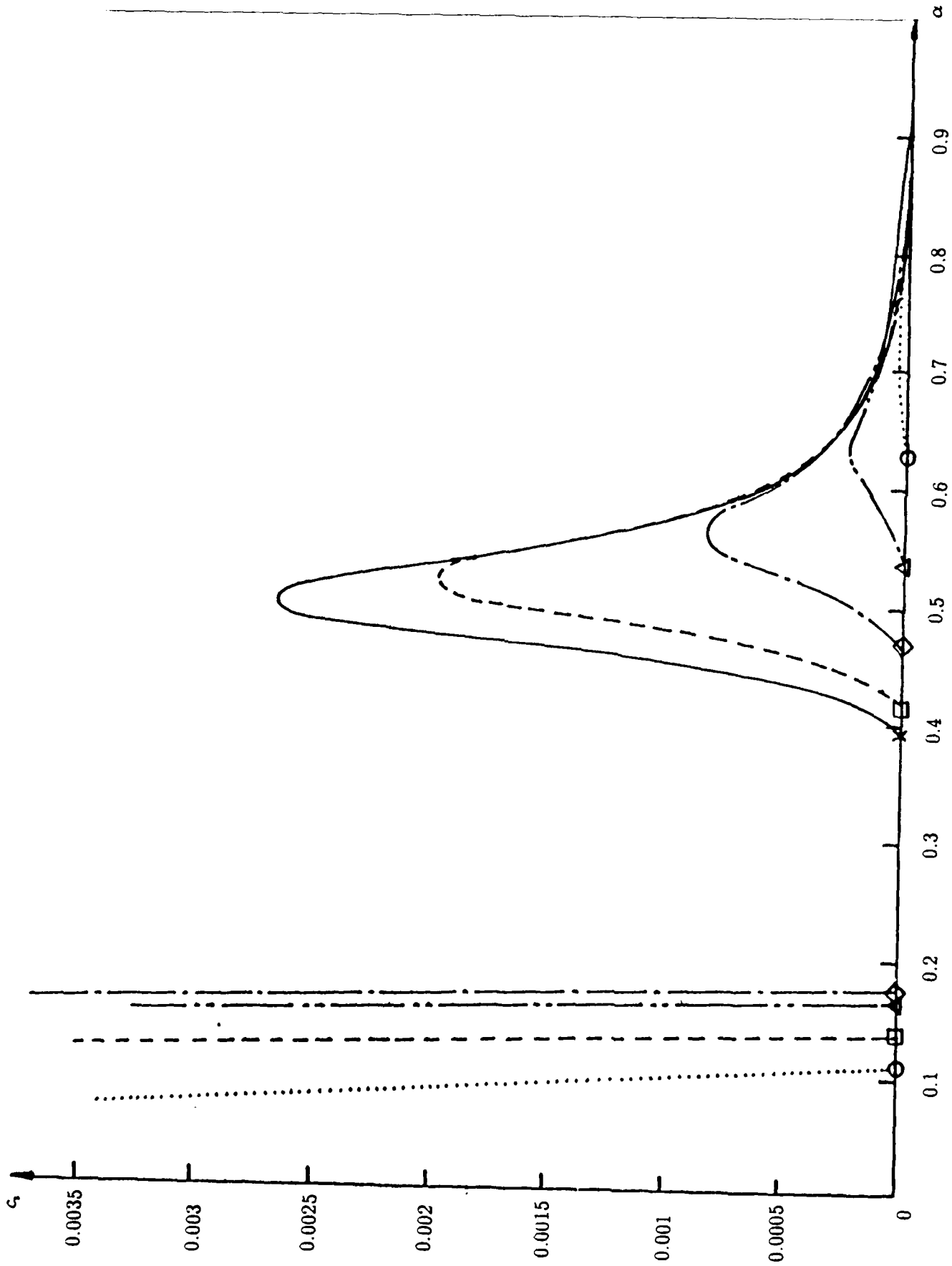


Fig.7b Details as Fig.7a, enlarged scale

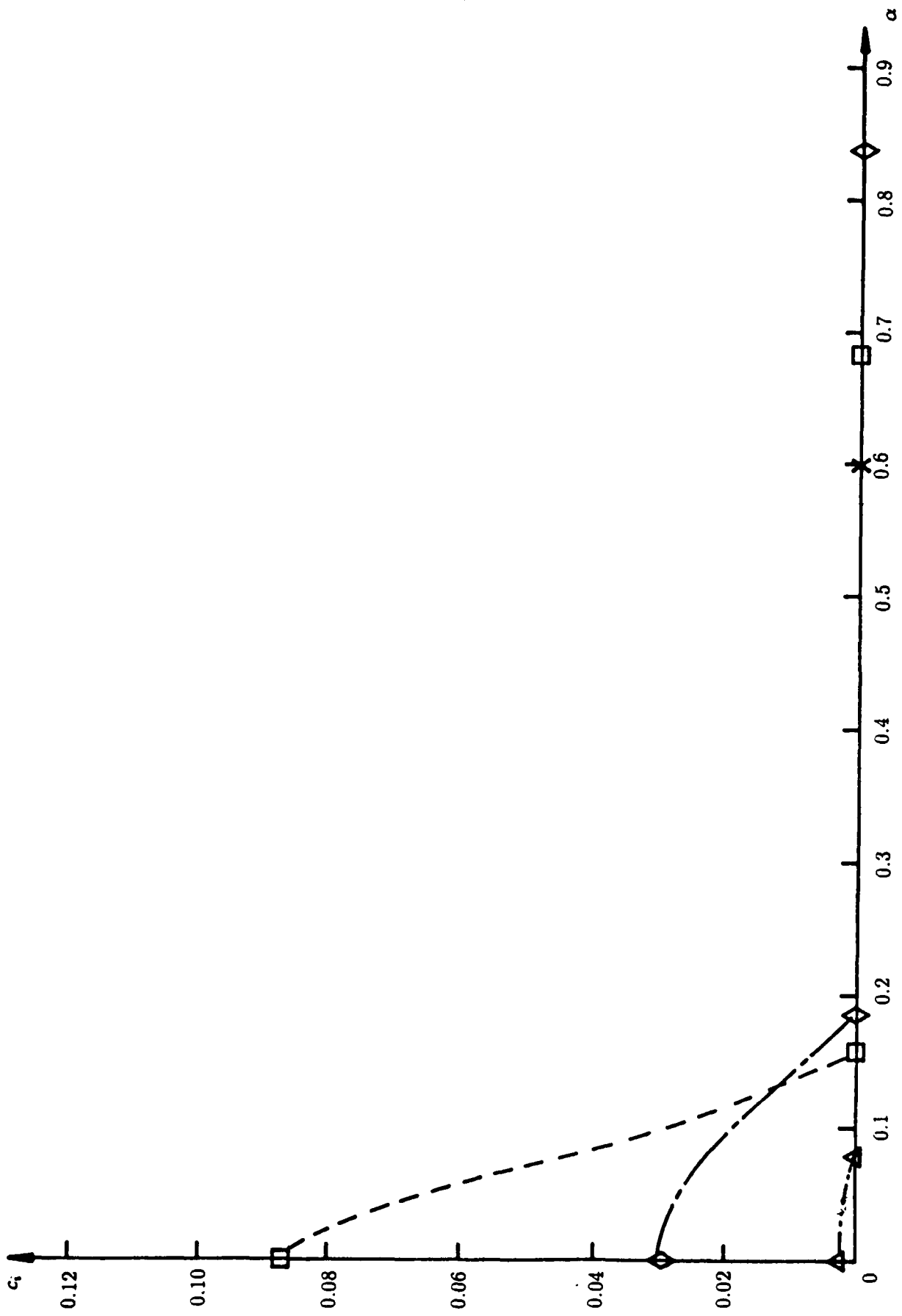


Fig. 8a Distributions of  $c_i$  with  $\alpha$ ,  $M_\omega = 3.8$ ,  $\zeta = 1.0$

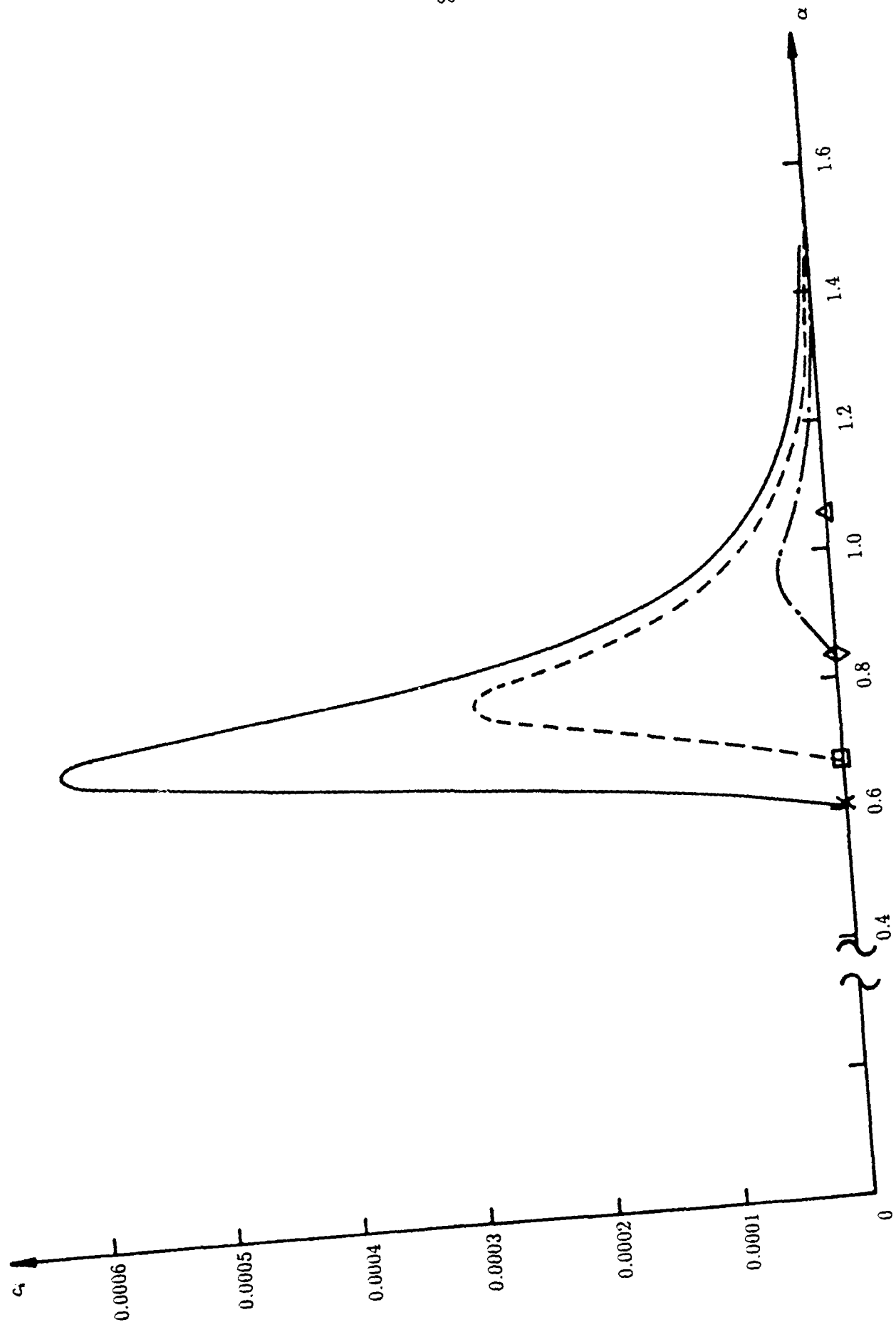


Fig. 8b Details as Fig. 8a, enlarged scale

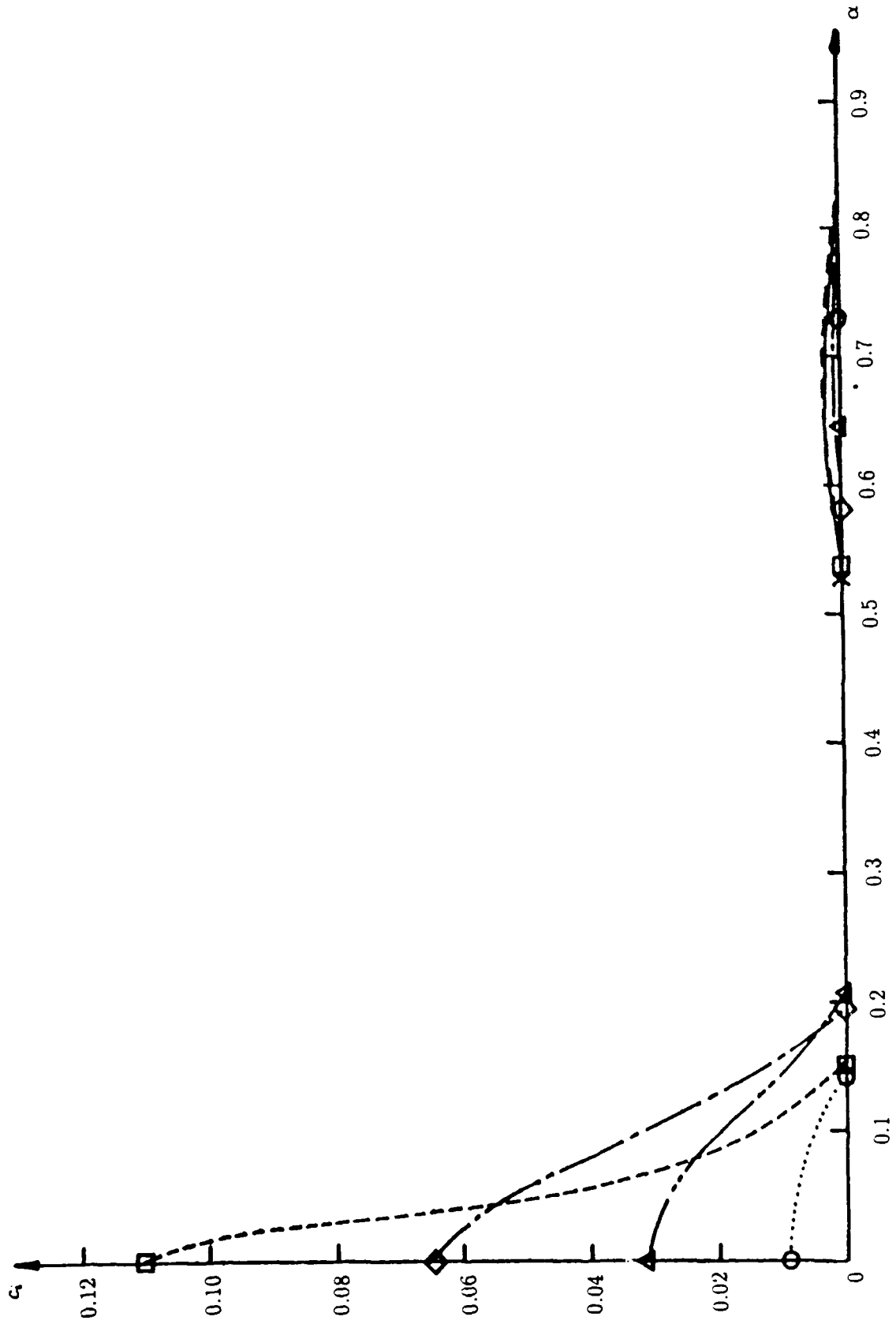


Fig. 9a Distributions of  $c_j$  with  $\alpha$ ,  $M_\infty = 3.8$ ,  $\zeta = 5.0$

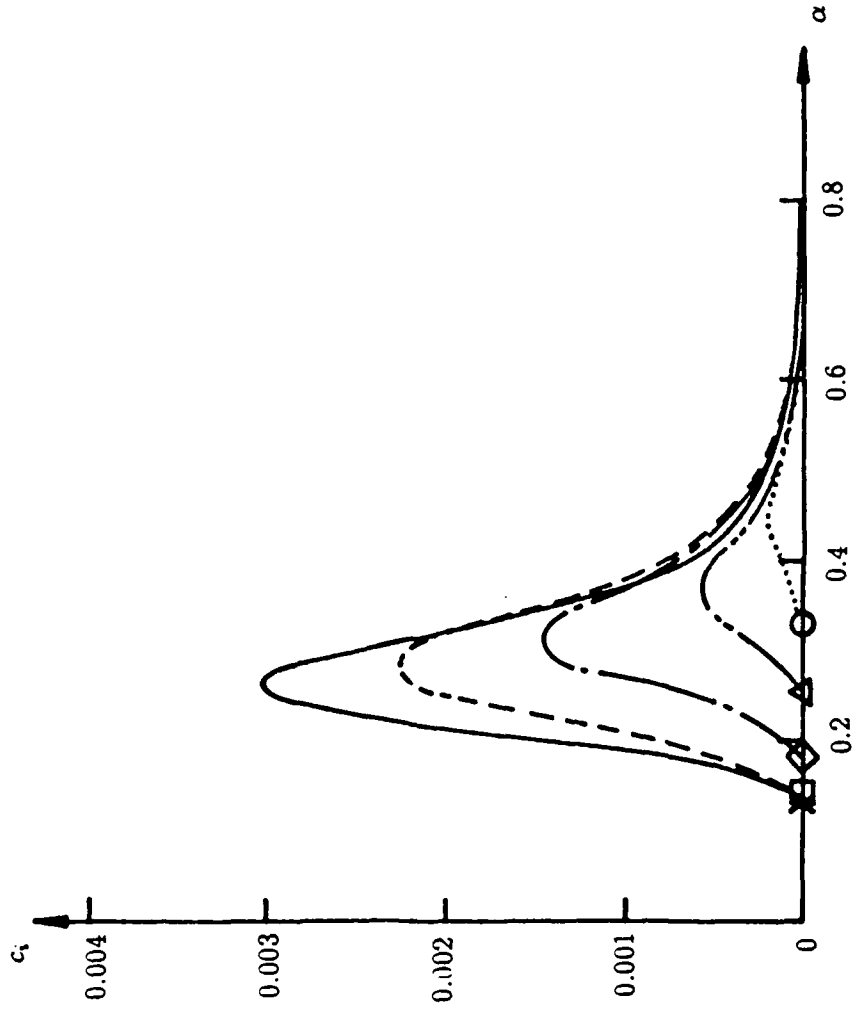


Fig.9b Details as Fig.9a, enlarged scale.

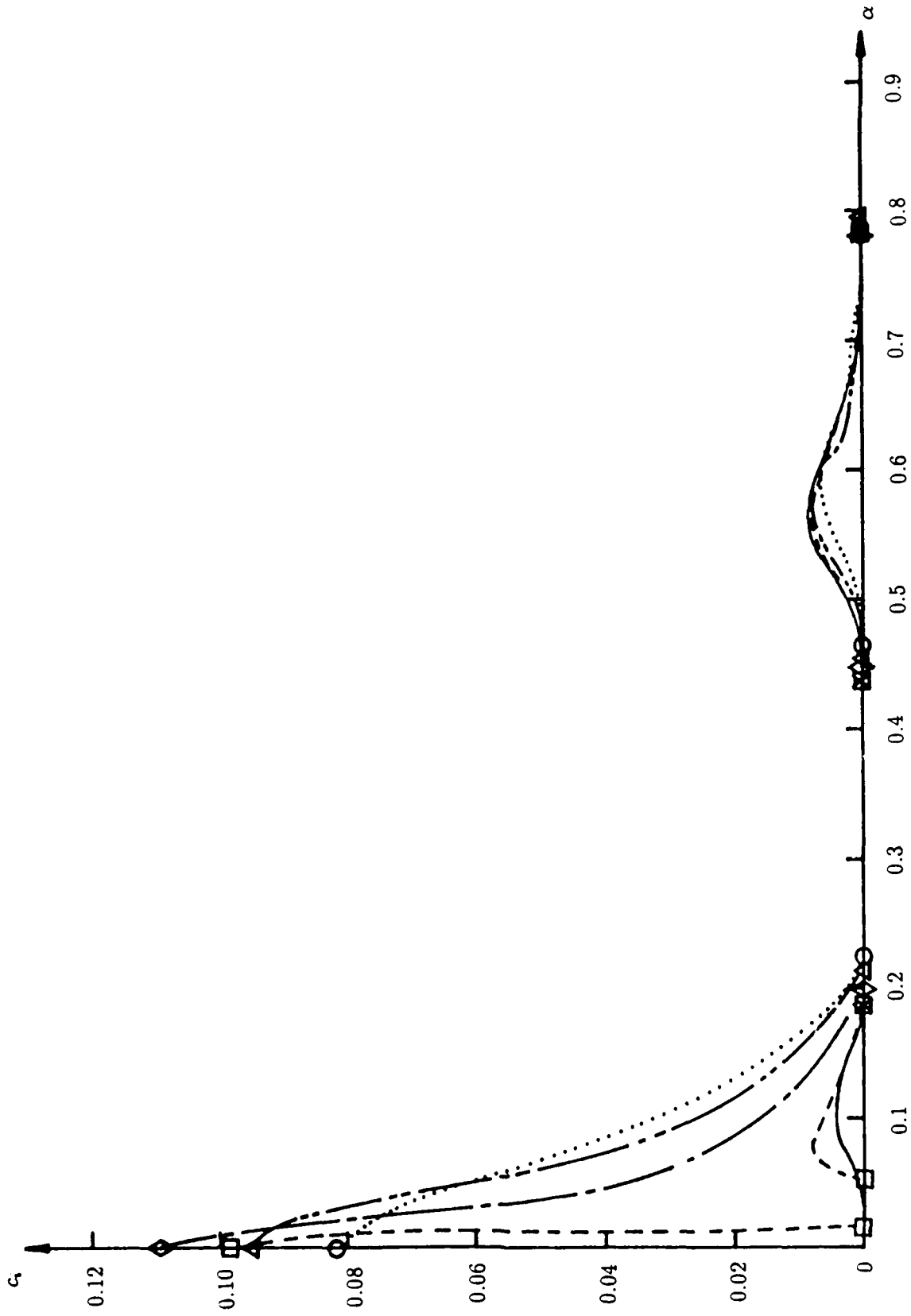


Fig.10 Distributions of  $c_j$  with  $\alpha$ ,  $M_\infty = 3.8$ ,  $\zeta = 20$

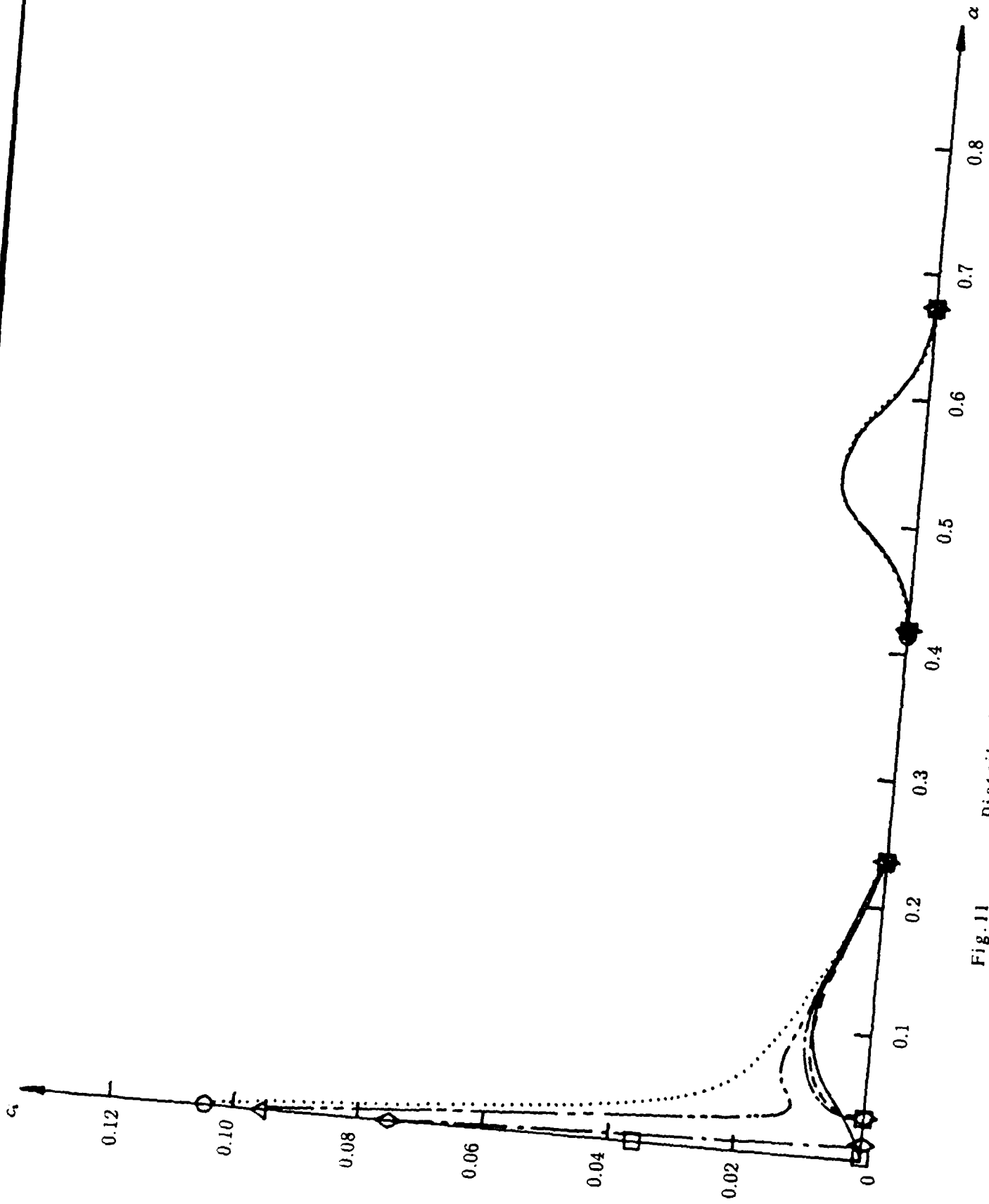


Fig. 11 Distributions of  $c_i$  with  $\alpha$ ,  $M_\omega = 3.8$ ,  $\zeta = 75$

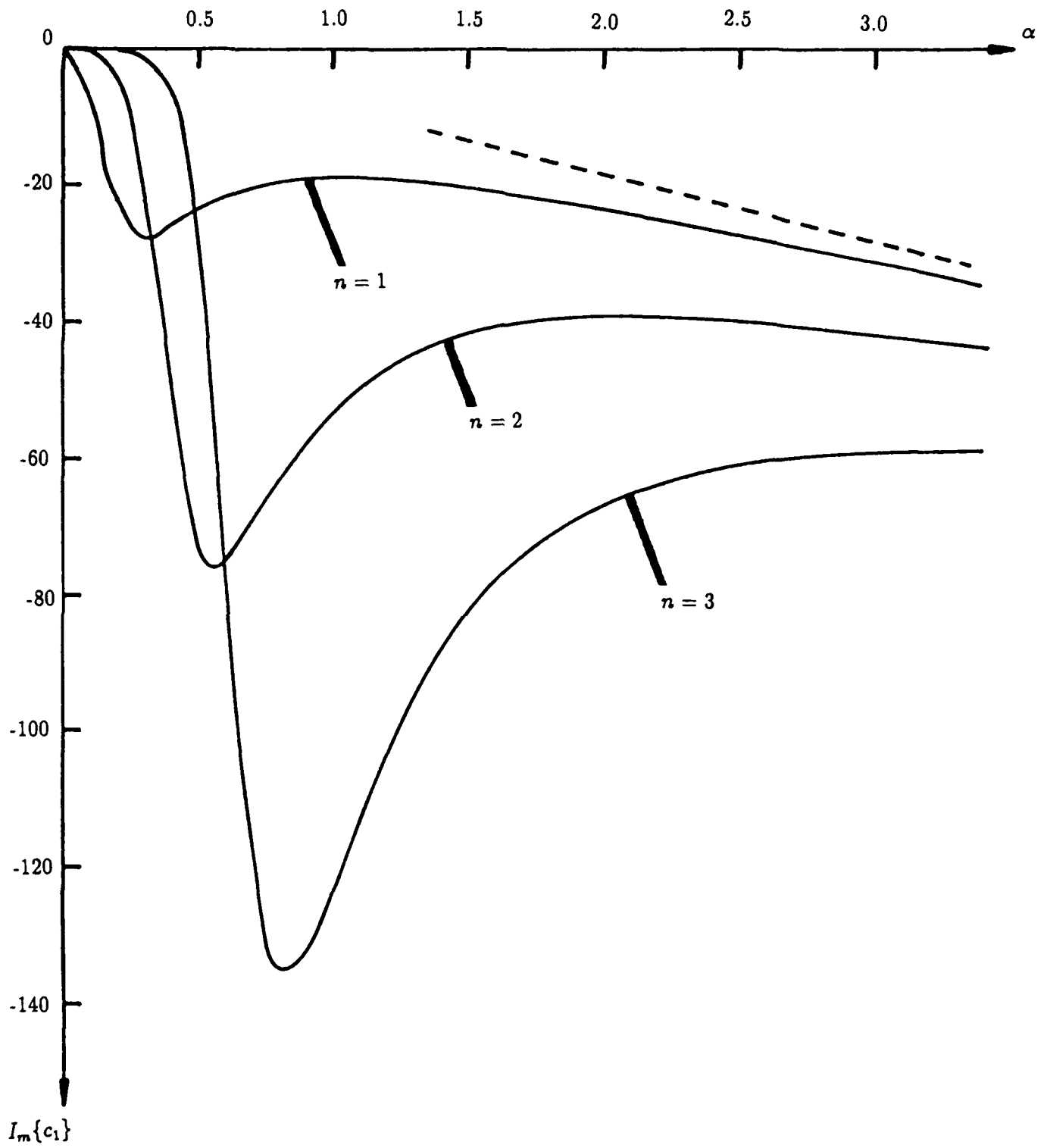


Fig. 12 Variation of  $\text{Im}\{c_1\}$  with  $\alpha$

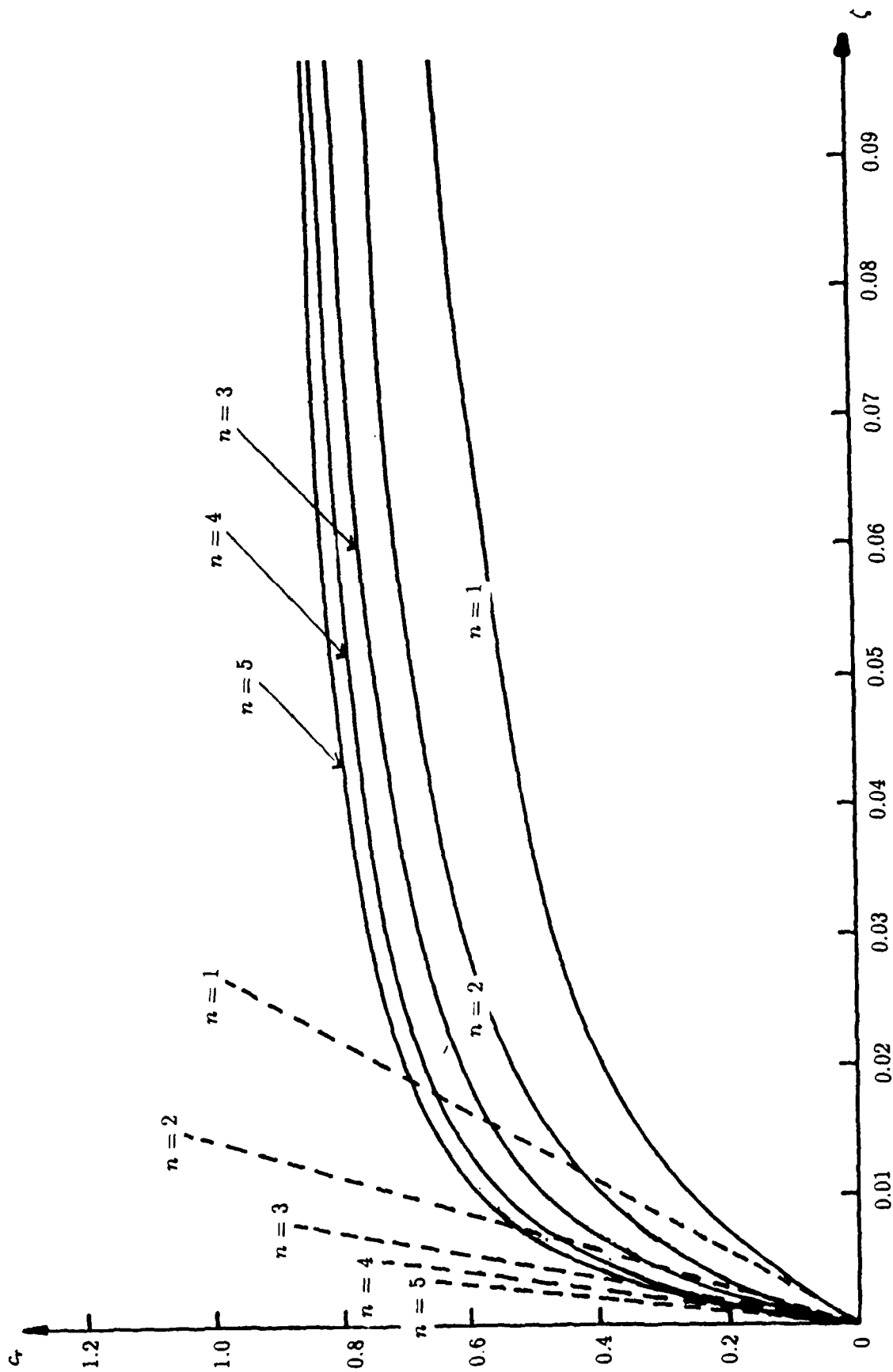


Fig. 13 Comparison of computed  $c_T(\alpha = 0)$  with asymptotic form

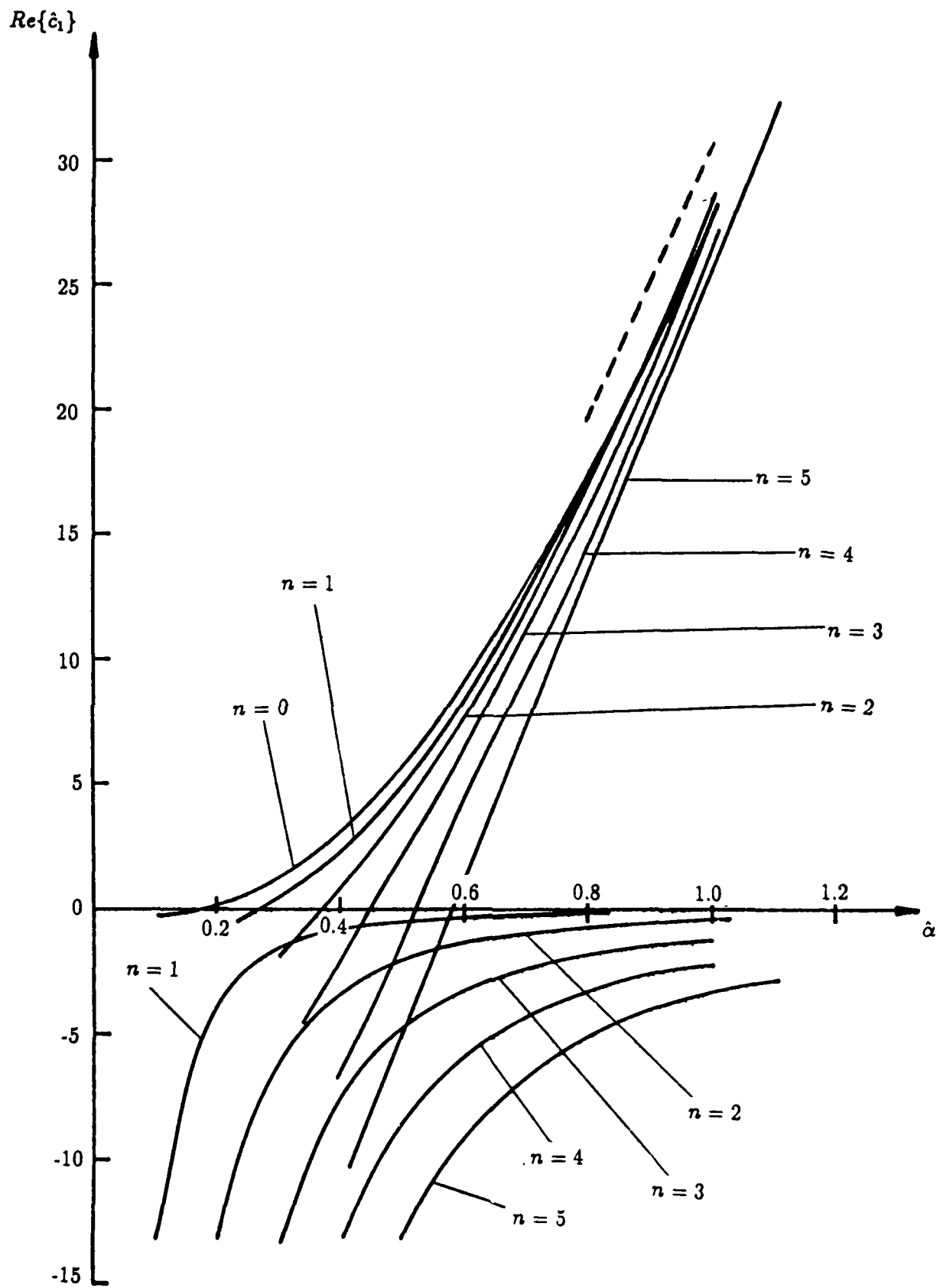


Fig. 14a Variation of Real  $\{\hat{c}_1\}$  with  $\hat{\alpha}$

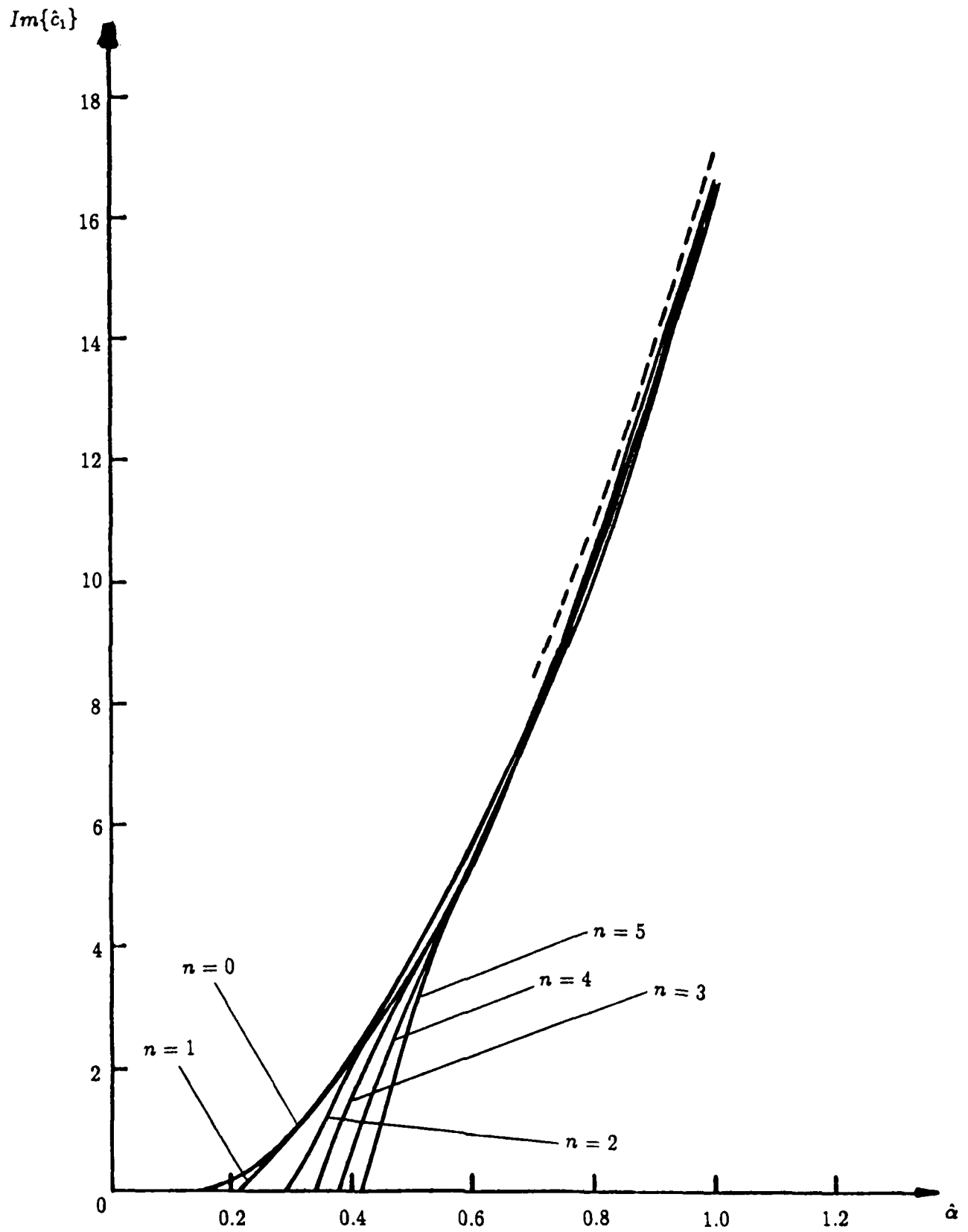


Fig. 14b Variation of  $Im\{\hat{c}_1\}$  with  $\hat{a}$



# Report Documentation Page

1. Report No. NASA CR-181996 ICASE Report No. 90-14	2. Government Accession No.	3. Recipient's Catalog No.	
4. Title and Subtitle  THE INVISCID STABILITY OF SUPERSONIC FLOW PAST A SHARP CONE	5. Report Date February 1990		
	6. Performing Organization Code		
7. Author(s)  Peter W. Duck Stephen J. Shaw	8. Performing Organization Report No. 90-14		
	10. Work Unit No. 505-90-21-01		
9. Performing Organization Name and Address Institute for Computer Applications in Science and Engineering Mail Stop 132C, NASA Langley Research Center Hampton, VA 23665-5225	11. Contract or Grant No. NAS1-18605		
	13. Type of Report and Period Covered Contractor Report		
12. Sponsoring Agency Name and Address National Aeronautics and Space Administration Langley Research Center Hampton, VA 23665-5225	14. Sponsoring Agency Code		
	15. Supplementary Notes  Langley Technical Monitor: Richard W. Barnwell  Final Report	Submitted to Theoretical & Computational Fluid Dynamics	
16. Abstract <p>In this paper we consider the laminar boundary layer which forms on a sharp cone in a supersonic freestream, where lateral curvature plays a key role in the physics of the problem.</p> <p>This flow is then analysed from the point of view on linear, temporal, inviscid stability. Indeed, the basic, non-axisymmetric disturbance equations are derived for general flows of this class, and a so called "triply generalised" inflexion condition is found for the existence of "subsonic" neutral modes of instability. This condition is analogous to the well-known generalised inflexion condition depends on both axial and aximuthal wavenumbers.</p> <p>Extensive numerical results are presented for the stability problem at a free-stream Mach number of 3.8, for a range of streamwise locations. These results reveal that a new mode of instability may occur, peculiar to flows of this type involving lateral curvature.</p> <p>Additionally, asymptotic analyses valid close to the tip of the cone / far downstream of the cone are presented, and these give a partial (asymptotic) description of this additional mode of instability.</p>			
17. Key Words Suggested by Author(s)  cone flow, inviscid stability, supersonic flow	18. Distribution Statement  02 - Aerodynamics  Unclassified - Unlimited		
19. Security Classif. of this report Unclassified	20. Security Classif. of this page Unclassified	21. No. of pages 60	22. Price A04